

Outside-xylem vulnerability, not xylem embolism, controls leaf hydraulic decline during dehydration

Christine Scoffoni^{1,2}, Caetano Albuquerque³, Craig R. Brodersen⁴, Shatara V. Townes¹, Grace P. John¹, Megan K. Bartlett¹, Thomas N. Buckley⁵, Andrew J. McElrone^{3,6}, Lawren Sack¹

¹ Department of Ecology and Evolutionary Biology, University of California Los Angeles, 621 Charles E. Young Drive South, Los Angeles, California, 90095, USA

² Department of Biology, Utah State University, Logan, UT 84322, USA

³ Department of Viticulture and Enology, University of California, Davis, CA 95616, USA

⁴ School of Forestry & Environmental Studies, Yale University, 195 Prospect Street, New Haven, CT 06511, USA

⁵ IA Watson Grains Research Centre, Plant Breeding Institute, Sydney Institute of Agriculture, The University of Sydney, Narrabri NSW 2390 Australia

⁶ USDA-Agricultural Research Service, Davis, CA 95616, USA

Corresponding Author:

Christine Scoffoni

University of California, Los Angeles

Department of Ecology and Evolutionary Biology

621 Charles E. Young Dr S, 90095 Los Angeles CA

Email: cscoffoni@ucla.edu

Phone: +001 310 206 2887

Contributions: CS, CB, AM, and LS designed experiments. CS, CA, ST, GJ, MB, TB, and AM performed experiments and simulations. CS, CA, and CB analyzed data. CS and LS wrote the manuscript with contributions from all authors.

One Sentence Summary: Changes in leaf outside-xylem properties drive leaf and whole plant hydraulic decline with dehydration, protecting plants from catastrophic embolism in xylem conduits.

Abstract

Leaf hydraulic supply is crucial to maintaining open stomata for CO₂ capture and plant growth. During drought-induced dehydration, the leaf hydraulic conductance (K_{leaf}) declines, which contributes to stomatal closure and eventually to leaf death. Previous studies have tended to attribute the decline of K_{leaf} to embolism in the leaf vein xylem. We visualized at high resolution and quantified experimentally the hydraulic vulnerability of xylem and outside-xylem pathways and modelled their respective influences on plant water transport. Evidence from all approaches indicated that the decline of K_{leaf} during dehydration arose first and foremost due to the vulnerability of outside-xylem tissues. *In vivo* x-ray micro-computed tomography of dehydrating leaves of four diverse angiosperm species showed that at turgor loss point only small fractions of leaf vein xylem conduits were embolized, and substantial xylem embolism arose only under severe dehydration. Experiments on an expanded set of eight angiosperm species showed that outside-xylem hydraulic vulnerability explained 75 to 100% of K_{leaf} decline across the range of dehydration from mild water stress to beyond turgor loss point. Spatially explicit modeling of leaf water transport pointed to a role for reduced membrane conductivity consistent with published data for cells and tissues. Plant-scale modeling suggested that outside-xylem hydraulic vulnerability can protect the xylem from tensions that would induce embolism and disruption of water transport under mild to moderate soil and atmospheric droughts. These findings pinpoint outside-xylem tissues as a central locus for the control of leaf and plant water transport during progressive drought.

Key words: aquaporins, bundle sheath cells, cavitation, drought, plant modelling

Introduction

Leaves account for the bulk of photosynthetic productivity and transpirational water use, and given the increasing incidence and severity of droughts in many regions (Vicente-Serrano et al., 2014; Diffenbaugh et al., 2015) if not globally (Sheffield et al., 2012), the mechanisms underlying the drought responses of leaves are ever more critical to understand. Reduction of photosynthesis and growth under mild dehydration and subsequent death under prolonged drought are primarily related to failure of the water transport system (Tyree and Zimmermann, 2002; Sack et al., 2016a). Water moves under negative pressure through plant xylem, via the “cohesion-tension” mechanism (Dixon and Joly, 1895), and a certain level of tension can cause air to aspirate through a xylem conduit causing spontaneous vaporization, a process known as “cavitation”. The resulting embolization of the xylem conduits has been widely believed to be the main cause of hydraulic decline during drought (Milburn, 1966; Tyree and Zimmermann, 2002), which results in declines in gas exchange rates (Nardini and Salleo, 2000; Brodribb and Holbrook, 2003; Hernandez-Santana et al., 2016), and can ultimately precipitate plant mortality (Choat et al., 2012). While embolism is a major cause of failure of stem hydraulic function, its role in leaves has yet not been clarified. Understanding the role of embolism on leaf hydraulic function is equally if not more important than in stems, as leaves represent a hydraulic bottleneck (Sack and Holbrook, 2006) that can determine plant hydraulic responses and the resulting declines in stomatal conductance and photosynthesis during drought (Brodribb and Holbrook, 2003; Sack and Holbrook, 2006). Leaves are highly vulnerable to dehydration, with leaf hydraulic conductance (K_{leaf}) often declining rapidly between full turgor and turgor loss point, and even more strongly during extreme dehydration (e.g., Brodribb and Holbrook, 2006; Johnson et al., 2009b; Scoffoni et al., 2012; Sack et al., 2016b). This response could arise in one or more of several tissues, as water moves first through the vein xylem, then exits the xylem through bundle sheath cells and flows through the mesophyll before evaporating into the intercellular air space, and diffusing through stomata out of the leaf (Figure 1) (Tyree and Yianoulis, 1980; Boyer, 1985; Rockwell et al., 2014). Thus, the decline of K_{leaf} with dehydration may be driven not just by reduced vein xylem hydraulic conductance (K_x), but also by reduced outside-xylem hydraulic conductance (K_{ox}), which includes pathways through vascular parenchyma, bundle sheath and the rest of the mesophyll tissues. Both K_x and K_{ox} determine K_{leaf} :

$$K_{\text{leaf}} = ((K_x^{-1} + K_{\text{ox}}^{-1})^{-1}) \quad \text{Eqn 1}$$

Indeed, recent studies have suggested that cell shrinkage with dehydration and/or deactivation of membrane aquaporins outside the xylem could strongly reduce K_{leaf} (Kim and Steudle, 2007; Shatil-Cohen et al., 2011; Pantin et al., 2013; Scoffoni et al., 2014; Moshelion et al., 2015; Sade et al., 2015). Yet, the vulnerability of K_x and K_{ox} , and their influences on K_{leaf} decline with dehydration have not been clearly disentangled. Though recent evidence has suggested that the leaf xylem is resistant to embolism under moderate levels of dehydration (Scoffoni and Sack, 2015; Bouche et al., 2016; Brodribb et al., 2016b), whole leaf hydraulic decline with dehydration has been most often primarily attributed to embolism, based on indirect evidence (e.g., Milburn and Johnson, 1966; Crombie et al., 1985; Kikuta et al., 1997; Nardini and Salleo, 2000; Salleo et al., 2000; Nardini et al., 2001; Salleo et al., 2001; Bucci et al., 2003; Lo Gullo et al., 2003; Nardini and Salleo, 2003; Nardini et al., 2003; Stiller et al., 2003; Trifilo et al., 2003a; Brodribb and Holbrook, 2005; Woodruff et al., 2007; Nardini et al., 2008; Johnson et al., 2009a; Blackman et al., 2010; Johnson et al., 2012; Blackman et al., 2014). For instance, the earliest report of xylem embolism was for leaf petioles, based on acoustic emissions thought to be caused by cavitation events (Milburn, 1966), and subsequent studies reported that the number of acoustic emissions a leaf generates correlated with leaf hydraulic decline (Tyree and Sperry, 1989; Johnson et al., 2009a). However, it is now recognized that acoustic emissions from drying leaves may arise from processes other than xylem conduit embolism, such as fractures in the tissues or embolism within fibers or mesophyll cell walls (Sandford and Grace, 1985; Ritman and Milburn, 1988; Cochard et al., 2013). In severely dehydrated excised leaves embolisms can be observed in the leaf vein xylem using scanning electron microscopy of cryogenized sections, dye methods or direct light transmission, and several studies reported that K_{leaf} decline corresponded to accumulation of leaf vein embolism (Cochard et al., 2000; Nardini et al., 2003; Trifilo et al., 2003b; Woodruff et al., 2007; Johnson et al., 2009a; Brodribb et al., 2016a), and suggested this to be the main driver of K_{leaf} decline. However, there has been a lack of information of the number of embolized xylem conduits within given vein orders across the range of leaf water stress and their influence on K_{leaf} (Wylie, 1947; McKown et al., 2010; Sack and Scoffoni, 2013) relative to the potentially strong role of vulnerability of the outside-xylem pathways. Recent work has proposed that outside-xylem hydraulic decline may play a role in K_{leaf} decline (Sade et al., 2014; Scoffoni et al., 2014; Hernandez-Santana et al., 2016; Trifilo et al., 2016). A recent study that partitioned the vulnerability of K_{leaf} into that of K_x and K_{ox} (Trifilo et al., 2016) found

that both contributed, depending on species, but measurements were made under low irradiance, which would minimize the response of K_{ox} before turgor loss point (Guyot et al., 2012; Sack et al., 2016b). A strong test of the relative roles of K_x and K_{ox} depends on their determination for illuminated leaves coupled with direct observations of the formation of emboli in the xylem.

To test the relative roles of xylem embolism and changes in outside-xylem properties in determining the decline in K_{leaf} during dehydration, we combined three approaches. We first investigated whether embolism occurred in leaf veins as leaves dehydrated to turgor loss and beyond using x-ray micro-computed tomography (microCT). We then quantified the vulnerability of K_x and K_{ox} to dehydration, which allowed us to partition their influence on the vulnerability of K_{leaf} at any point during dehydration under high irradiance. We investigated the anatomical determinants of the decline in outside-xylem pathways using a spatially explicit model of leaf water transport. Finally, we tested the implications of our findings, using model of the whole plant hydraulic system to estimate the influence of the measured declines of K_x , K_{ox} and K_{leaf} on whole plant hydraulic conductance under different drought scenarios.

Results

The main determinant of K_{leaf} decline in dehydrating leaves was hydraulic vulnerability of the outside-xylem pathways rather than xylem embolism, for eight angiosperm species from eight families (Table 1). The strong declines of K_{leaf} during progressive dehydration above and below turgor loss point did not reflect patterns of xylem embolism observed *in vivo* (Figures 2-3). MicroCT imaging of dehydrating leaves of four species revealed few gas-filled conduits even at the turgor loss point, and at leaf water potentials at which K_{leaf} had already declined by over 60% (Figures 2-3) where on average only 5 to 8.5% of midrib conduits were embolized across species in the midrib and none in the minor veins (Table 2). Substantial levels of embolism (a maximum of 44% across species) were observed in the midrib only under extreme dehydration beyond the turgor loss point (Table 2), but emboli were non-existent or rare in the minor veins of these species at those extreme water potentials (Scoffoni et al., 2016). Hydraulic measurements of K_x vulnerability across the four species used for microCT imaging and an additional four ecologically diverse species (Table 1) corroborated the microCT evidence of low K_x vulnerability on average across species compared to K_{leaf} . Thus, the water potential inducing

50% loss of hydraulic conductance for the leaf xylem ($P_{50,Kx}$ obtained from K_x vulnerability curves shown in Figure S1) was on average 1.6 MPa more negative than that for the whole leaf ($P_{50,Kleaf}$; Figure 3), representing a much lower sensitivity to water stress of K_x than of either K_{leaf} or K_{ox} (p -values of 0.015 and 0.007 respectively; paired t -tests for each species; values for $P_{50,Kx}$, $P_{50,Kox}$ and $P_{50,Kleaf}$ are shown in Table 1). By contrast, the water potential inducing 50% loss of hydraulic conductance for the outside-xylem pathways ($P_{50,Kox}$) was on average 0.1 MPa less negative than $P_{50,Kleaf}$, representing only a slightly greater sensitivity. Although the vulnerability of K_x to dehydration was much smaller than that of K_{ox} for all species, their relative sensitivities varied: the $P_{50,Kx}$ ranged from only 0.08-0.8 MPa more negative than $P_{50,Kox}$ in two soft-leaved shrub species (*Lantana camara* and *Salvia canariensis*), to 2.9-3.2 MPa more negative in sclerophyllous species of the California chaparral (*Comarostaphylis diversifolia* and *Quercus agrifolia*). Partitioning the contributions of xylem and outside-xylem pathways to the decline of K_{leaf} (see *Methods*) showed that across species, the decline in K_{ox} explained 86 to 100% of the decline in K_{leaf} at turgor loss point (96% on average across species), 95 to 100% of that at $P_{50,Kleaf}$ (98% on average) and 75 to 100% of that at water potentials inducing 88% loss of leaf hydraulic conductance ($P_{88,Kleaf}$; 93% on average; Table 3). Further, while across species both $P_{50,Kx}$ and $P_{50,Kox}$ correlated positively with $P_{50,Kleaf}$ ($r^2 = 0.57$ and 0.99 respectively), when testing models predicting $P_{50,Kleaf}$ from $P_{50,Kox}$ and/or $P_{50,Kx}$, the model with $P_{50,Kox}$ alone was selected by maximum likelihood as the better predictor (Table S1), explaining 81% of $P_{50,Kleaf}$ variation across species according to independent effects analysis.

Our model simulations of the plant hydraulic-stomatal system showed that on average across species (Figure 4), and for 3 of 4 species individually (Figure S2; Table S2), decline of K_{ox} would be the main determinant of the decline of not only K_{leaf} but of whole plant hydraulic conductance under a wide range of scenarios of atmospheric drought (i.e., high VPD) or soil drought (i.e., increasingly negative soil water potentials, Ψ_{soil}). Indeed, the trajectory of the percent loss of conductivity of the whole plant hydraulic system to either type of drought showed strong overlap with that of K_{ox} , while the bottleneck imposed by low K_{ox} shielded the leaf and stem xylem hydraulic conductances from tensions that would result in significant declines in these components under increasing VPD or increasingly negative Ψ_{soil} . Roots also have water flowing through living tissues outside-xylem component, and root hydraulic conductance (K_{root}) shows steep hydraulic vulnerability (Brodribb and Hill, 2000; Hacke et al., 2000; North et al.,

2004), but K_{root} too is shielded from decline under increasing VPD by the bottleneck imposed by declining leaf K_{ox} . Notably, like the other compartments, K_{root} strongly declines under more negative Ψ_{soil} . However, because Ψ_{soil} is less negative than leaf water potential during transpiration, K_{root} does not decline as strongly as leaf K_{ox} on average across species. Even for *Lantana camara*, which has relatively vulnerable xylem, under increasing VPD, the decline of K_{ox} is steep and protects the other compartments of the plant from high tensions as for the other species, though under soil drought, steep declines in hydraulic conductances would occur in all organs (Figure S2). Across species, the vulnerability of the hydraulic pathways correlated with the drought tolerance of the mesophyll cells. Thus, bulk leaf turgor loss point (Ψ_{TLP}) correlated with $P_{50,K_{\text{ox}}}$ and $P_{50,K_{\text{x}}}$ ($r^2 = 0.69$ and 0.91 respectively, $p \leq 0.01$).

We applied models to refine hypotheses for the source of the decline of K_{ox} in dehydrating leaves. We parameterized the MOFLO model for water transport outside the xylem (Buckley et al., 2015) with shifts in leaf anatomy and physiology that can be directly observed or that were experimentally determined or hypothesized in the literature to occur during dehydration, including leaf and internal tissue shrinkage, cell wall shrinkage, reduction in cell connectivity and decreases in membrane permeability (Sancho-Knapik et al., 2011; Shatil-Cohen et al., 2011; Pou et al., 2013; Scoffoni et al., 2014; Sade et al., 2015), and with or without assuming an apoplastic barrier at the bundle sheath as has been reported for some species (Lersten, 1997; Taneda et al., 2016). Across all four species, a reduction of membrane permeability in the context of an apoplastic barrier was the only factor that could directly account for decline of K_{ox} values during dehydration. Model simulations showed that an 80% reduction in membrane permeability in the context of an apoplastic barrier resulted in 58 to 86% decline of K_{ox} values. However, without an apoplastic barrier, the decrease of K_{ox} due to membrane permeability reduction would not be important enough to overcome the opposing effect of tissue shrinkage. Notably, leaf and tissue shrinkage as measured from microCT images (Figure 5) would, by itself, actually *increase* K_{ox} by 4 to 55 % across species, by shortening flow pathways outside the xylem (Figure 6). Further, An 80% reduction in cell connectivity had little impact, and in most cases (especially under the “no apoplastic barrier” scenario) its decrease was not sufficient to overcome the increase in K_{ox} induced by cell shrinkage (Figure 6). Notably, an 80% reduction in cell wall thicknesses yielded reductions in K_{ox} regardless of simulating an

apoplastic barrier or not, with 11-72% declines in K_{ox} at turgor loss point across species and scenarios.

Discussion

Vulnerable outside-xylem pathways protect the xylem from embolism throughout the plant

Our results from both microCT imaging and hydraulics experiments suggest the primary determinant of K_{leaf} decline in leaves from mild to extreme dehydration originated in vulnerability of the outside-xylem pathways, and not hydraulic failure of the xylem. Across species, the decline in K_{ox} caused >85% of the decline in K_{leaf} for water potentials by the turgor loss point, and > 75% by $P_{88}K_{leaf}$. These results are consistent with the body of literature linking changes in aquaporin expression to leaf hydration status and bundle sheath and mesophyll cell turgor (see below; Johansson et al., 1998; Kim and Steudle, 2007; Miyazawa et al., 2008; Kim and Steudle, 2009; Shatil-Cohen et al., 2011; Shatil-Cohen and Moshelion, 2012; Pou et al., 2013; Prado and Maurel, 2013; Laur and Hacke, 2014; Scoffoni et al., 2014; Sade et al., 2015). Our results are also consistent with those of two recent studies using an optical transmission approach, which found that long dehydrating times (up to 70h) and very negative water potentials below turgor loss point were necessary before vein embolisms were observed in leaf veins (Brodribb et al., 2016a; Brodribb et al., 2016b). One of those studies showed a correlation between vein embolism and K_{leaf} decline in four species (Brodribb et al., 2016a), though this was not necessarily causative as K_{leaf} appeared to decline by up to 50% before turgor loss point and before any signal of embolism in leaf veins. Additionally, the sensitivity of K_{ox} and K_{leaf} may have been stronger under high irradiance than assessed in that study in which leaves were acclimated under low irradiance ($<100 \mu\text{mol quanta m}^{-2} \text{s}^{-1}$), as for many species, K_{leaf} in hydrated leaves can be enhanced by many fold under high irradiance likely due to aquaporin expression (e.g., Cochard et al., 2007; Scoffoni et al., 2008; Maurel et al., 2015) and such high-light acclimated leaves show stronger vulnerability before turgor loss point (Guyot et al., 2012; Sack et al., 2016b). Similarly, a recent study partitioning the vulnerabilities of K_x and K_{ox} found that K_{ox} was the strongest determinant of K_{leaf} decline in 2/4 species (Trifilo et al., 2016) and for the other two species, both xylem and outside-xylem pathways appeared to be strong drivers of

K_{leaf} decline. However, hydraulics measurements were performed in that study under low light, likely minimizing the response of K_{ox} before turgor loss point.

Indeed, our results for angiosperm leaves with their complex venation may be general for a yet greater diversity of plants, as two recent studies using microCT on needles of *Pinus pinaster* found few embolized conduits at needle water potentials that induced strong declines in K_{leaf} (Charra-Vaskou et al., 2012; Bouche et al., 2016).

These findings suggest that the leaf outside-xylem pathways, in addition to experiencing the most negative water potentials in the plant, also have very strong hydraulic vulnerability. Such results are consistent with the hypothesis that strong K_{ox} declines would act as a protective bottleneck, shielding the leaf and stem xylem under many scenarios of atmospheric and soil drought from tensions that would induce catastrophic embolisms (Scoffoni et al., 2014). Further mechanisms for protection may operate additionally; a recent study found that minor vein collapse in leaves of red oak occurred under very strong tensions ($< -3\text{MPa}$) below turgor loss point and could thus act as a further buffer against embolism under prolonged drought (Zhang et al., 2016). Notably, a similar protection occurs in roots, as cortical lacunae formation in fine roots induced strong declines in hydraulic conductance protecting root xylem conduits from embolism formation (Cuneo et al., 2016). Such a strong role of outside-xylem pathways in hydraulic decline in both leaves and roots suggests a general advantage throughout the plant of sensitive living tissues protecting the xylem from catastrophic embolism. Given that stem embolism may be in many or most cases irreversible (Urli et al., 2013), such a protective effect would be most important for long-lived leaves and stems with high carbon investment, as commonly found in many drought prone systems such as chaparral communities. This hypothesis of the importance of K_{ox} response was supported by our model simulations showing that whole plant hydraulic conductance would decline under increasing soil drought and/or atmospheric drought (i.e., high vapor pressure deficit, VPD) primarily as a consequence of the strong declines in K_{ox} . Because the leaves experience the lowest water potentials, and declining K_{ox} provides an increasing bottleneck in the system, the tensions developed in leaf and stem xylem were in most modeled scenarios insufficient to cause catastrophic embolism. The declines in K_{ox} and K_{leaf} may further protect the stem xylem from strong tensions and embolism if the strongly declining water potentials in the mesophyll influence stomatal closure, which tends to begin well above bulk leaf turgor loss point (Ψ_{TLP}) (Bartlett et al., 2016), K_{ox} could be playing an

important role in stomatal control. Another potential advantage of outside-xylem pathways being more sensitive to dehydration is that they might recover more rapidly with water potential than embolized conduits in the xylem. Thus, changes in outside-xylem pathways with dehydration could be more reversible during drought and recovery cycles than xylem embolism. While xylem embolism requires several hours under no tension to recover by capillarity (Hochberg et al., 2016; Knipfer et al., 2016), in some species K_{leaf} can partially recover after only 1h of rehydration in some species (Scoffoni et al., 2012), which could be due to recovery of K_{ox} . Future work should resolve the influence of K_x and K_{ox} decline on stomatal conductance and their recovery.

These results provide strong evidence for the role of outside-xylem pathways in driving changes in K_{leaf} and whole plant conductance under the range of water potential plants experience through mild and moderate drought stress. In contrast, after stomatal closure and under conditions of prolonged drought, sustained dehydration will induce embolism in leaf veins and likely in the stem xylem, eventually contributing to hydraulic failure and plant death (Anderegg et al., 2015).

Determinants of outside-xylem hydraulic conductance decline with dehydration

Given the key role of K_{ox} decline in dehydrating leaves, resolving the underlying causes is crucial. Experimental investigation remains challenging not only because of the complexity of liquid water movement through the living tissues outside the vein xylem, but also because vapor-phase pathways contribute to K_{ox} and thus K_{leaf} (Pieruschka et al., 2010; Rockwell et al., 2014; Buckley et al., 2015). We implemented a spatially explicit model for the anatomical and biophysical determination of K_{ox} (MOFLO; Buckley et al., 2015), and parameterized the model with our measurements of tissue structure in dehydrating leaves. These simulations showed that shrinking cells and airspaces in dehydrating leaves would in fact act to *increase* K_{ox} due to the effects of shorter pathlengths for water transport to the stomata both horizontally as effective vein length per leaf area increases, and vertically from vein to stomata given the shrinkage of the leaf thickness. Simulations showed that declines in membrane permeability could be important determinants of K_{ox} decline which would drive K_{leaf} decline overall, despite the effect of reduced tissue dimensions. A decline in membrane permeability could result from reduced aquaporin

activity as cells dehydrate, a response previously demonstrated in studies using mutants of the model species *Arabidopsis thaliana* and in cell probe studies of *Zea mays* (Johansson et al., 1998; Kim and Steudle, 2007; Maurel et al., 2015). Further, previous studies have found either aquaporin mutants or leaves of species previously perfused with aquaporin inhibitors to exhibit up to 75% decrease of K_{leaf} (Shatil-Cohen et al., 2011; Pou et al., 2013; Sade et al., 2015). Our findings are in line with the hypothesis that reduced aquaporin activity, potentially triggered by turgor decline and/or abscisic acid (ABA) production during dehydration, would drive K_{ox} decline (Shatil-Cohen et al., 2011), and further suggest that such a response would scale up to determining decline of K_{leaf} and whole plant hydraulic decline. We found that to model the observed declines of K_{ox} due to reduction of membrane permeability, it was necessary to posit an apoplastic barrier at the bundle sheath, analogous to the Casparian strip in root endodermis (Canny, 1986, 1988), to constrain all water to exit the veins via bundle sheath cell membranes rather than via the apoplast. Such an apoplastic barrier has previously been supported by dye experiments (Shatil-Cohen et al., 2011; Shatil-Cohen and Moshelion, 2012) and hydraulics measurements on other species (Sack et al., 2004; Sade et al., 2014), and visualized in anatomical studies of some, but not all species tested (Canny, 1986; Lersten, 1997; Wu et al., 2005; Ribeiro et al., 2007; Taneda et al., 2016). The restriction of water movement needed to explain declines in K_{ox} could occur at the site at which water exits vascular parenchyma to reach bundle sheath cells or cell walls, or via a forced symplastic flow path through the vascular parenchyma cells until it reaches the bundle sheath; any of these mechanisms would strongly increase the resistance in water movement (Buckley, 2015). Elucidating whether such apoplastic barriers or symplastic flows through vascular parenchyma are typical is an important topic for future studies. Finally, modeling showed that changes in cell wall thickness during dehydration could strongly influence K_{ox} (Figure 6), given the important contribution of apoplastic cell wall pathways through the mesophyll in determining K_{ox} at full hydration (Buckley, 2015). However, such putative changes in cell wall thickness with dehydration have never been documented to our knowledge. Our results, along with the numerous aquaporin studies (see references above), most strongly support changes in membrane permeability at the vascular parenchyma or bundle sheath cell level as a mechanism for decline in K_{ox} with dehydration.

Across species, K_{ox} and K_x vulnerability during leaf dehydration correlated strongly with bulk leaf turgor loss point (Ψ_{TLP}). The Ψ_{TLP} is a good indicator of species drought tolerance

across ecosystems, with more negative values present in species occurring in drier habitats or ecosystems (Bartlett et al., 2012). Recently, several studies have shown strong correlation of $P_{50,K_{leaf}}$ with Ψ_{TLP} across diverse angiosperm species (e.g., Blackman et al., 2010; Scoffoni et al., 2012). These studies hypothesized that cells maintaining turgor at more negative water potentials could preserve cell integrity and thus hydraulic pathways outside the xylem, and thus confer resistance to hydraulic decline. However, given that our model simulations revealed that cell shrinkage would not cause a decline in K_{ox} as previously hypothesized (Scoffoni et al., 2014), an indirect mechanism must underlie this correlation; for instance, a more negative Ψ_{TLP} may correspond to a greater ability to maintain cell membrane permeability especially in the vascular parenchyma and/or bundle sheath (Kim and Steudle, 2007). The hypothesis that cell turgor loss might trigger aquaporin deactivation and/or ABA production (Pierce and Raschke, 1980; Shatil-Cohen et al., 2011), which in turn would reduce membrane permeability, is consistent with recent work on cells and tissues in a range of species (Wan et al., 2004; Ye et al., 2005; Kim and Steudle, 2007; Shatil-Cohen et al., 2011; Brodribb and McAdam, 2013; Chaumont and Tyerman, 2014; McAdam and Brodribb, 2014; Vandeleur et al., 2014). Another source of the coordination of Ψ_{TLP} with the hydraulic vulnerability of the leaf and its compartments is that all of these physiologically important traits are co-selected in species with greater drought tolerance (Blackman et al., 2010; Bartlett et al., 2012; Blackman et al., 2014; Bartlett et al., 2016).

Conclusion

Combining empirical, visual and modeling approaches, we found that in 8 diverse species the observed decline in leaf hydraulic conductance during mild dehydration results primarily from losses in hydraulic conductance outside the vascular system (>75% across leaf dehydration from mild to extreme; 96% on average). These results indicate that outside-xylem processes are the main determinants of K_{leaf} vulnerability to dehydration. Leaves avoid catastrophic xylem failure by regulating their outside-xylem hydraulic conductance. After stomatal closure and under extreme drought, leaf vein and stem embolism might be unavoidable and induce catastrophic hydraulic failure. These findings pinpoint the mesophyll tissues including bundle sheath as a central locus for the control of leaf and plant water transport during progressive drought.

Material and Methods

Plant material

Measurements were obtained for eight species diverse in phylogeny, origin, drought tolerance and life form (Table 1), growing in and around the campus of the University of California, Los Angeles, and Will Rogers State Park. Measurements were conducted from November 2013 to November 2014. The day before any of the measurements described below, shoots with a minimum of three nodes of stem below the leaves to be studied were excised in air from at least three individuals, and transported in dark plastic bags filled with wet paper towels, where the shoot was re-cut underwater by a minimum of two nodes from the base and left to rehydrate overnight. We note that though obtained in different years, both leaf and xylem hydraulic vulnerability curves were obtained from the same individuals, and no differences were found in K_{leaf} values across years (Scoffoni et al., 2011; Guyot et al., 2012).

X-ray microtomography

To directly visualize embolism in the xylem and structural changes in all orders of veins and in the mesophyll tissues, we used high-energy, high resolution X-ray micro-computed tomography (microCT) at the synchrotron at the Advanced Light Source (ALS) in Berkeley, California (Beamline 8.3.2) in November of 2014. Stacks of images were obtained by scanning the center (including the mid-vein) of living leaves on dehydrating shoots for four of our study species (*Comarostaphylis diversifolia*, *Hedera canariensis*, *Lantana camara* and *Magnolia grandiflora*). Species were chosen for microCT based on their wide range of drought tolerance. Detailed description of sample preparation for microCT imaging is discussed in Supplementary Material and Methods. Nine to twelve scans of the midrib and surrounding mesophyll at the center of leaf were made per species of leaves spanning the whole range of leaf water potential obtained in the K_x vulnerability curves (described below).

On three cross-sectional images randomly selected at the bottom, middle and top part along the main axis of the microCT scan, conduit embolism in the midrib, along with mesophyll cell and tissue dimensions were quantified. For each image we measured the number of embolized conduits in the midrib and averaged for three areas of the leaf lamina measurements of the dimensions of tissues and cells (epidermis and cuticle, palisade mesophyll, spongy mesophyll, and palisade cell area, height and diameter) using ImageJ software (version 1.46r; National Institutes of Health). Bundle sheath thickness and cell dimensions could not be

resolved in these images. Three-dimensional volume renderings of our scans were made using Avizo 8.1.1 software (VSG, Inc., Burlington, MA, USA), and used to determine the vein orders (identified by following the branching pattern from the secondary veins), and cross-sectional images at the start, middle and end of the scanned region were used to determine the number of embolized conduits.

We calculated the percent number of embolized conduits in the midrib (%EMC) at given leaf water potentials. Embolized conduits appear brightly in the images, but non-embolized conduits cannot be distinguished from each other or counted. Thus, we estimated the total number of midrib conduits in cross-sections of these leaves using data taken from cross-sections of three leaves sampled from the same plants of each species and visualized by light microscopy (Figure S3; see *Light microscopy of cells and tissues within leaves* section below for methods). Given that the number of midrib xylem conduits scales with the midrib vascular cross-sectional area for well hydrated leaves of given species (Coomes et al., 2008; Taneda and Terashima, 2012), we counted the total number of xylem conduits in the midrib cross-sections obtained from light microscopy for hydrated leaves and normalized by their midrib vascular area. These were averaged for each species to determine conduit number per vascular area for hydrated leaves (CNA_{hydr}). Cross sections for both light microscopy and microCT scans were taken at the leaf midrib center. To calculate the total number of midrib conduits in cross-sections of the scanned dehydrated leaves (CNA_{dehydr}) we had to account for the shrinkage of the midrib vascular area with water potential. For the scanned dehydrated leaves of each species, we plotted midrib vascular area for the dehydrated leaves (A_{dehydr}) and for the three fully hydrated leaves measured using light-microscopy against leaf water potential (Figure S4) and thus estimated the proportion area shrinkage relative to the value extrapolated to 0 MPa for each leaf (AS_{dehydr}). Conduit number for each individual scanned leaf was obtained as:

$$CN = CNA_{hydr} \times \frac{A_{dehydr}}{(1-AS_{dehydr})} \text{ eqn 2,}$$

We counted the number of embolized conduits in each scanned leaf (CN_{emb}) and calculated % EMC as:

$$\% EMC = \frac{CN_{emb}}{CN} \times 100 \quad \text{eqn 3}$$

We note that the %EMC values differ slightly from those previously reported for the same images (Scoffoni et al., 2016), as we improved the calculation by adding the areas of the

three light-microscopy images of fully hydrated leaves to the regression against water potential to determine AS_{dehydr} . This improved calculation resulted in no major changes in the patterns observed.

We considered the potential concern that the x-ray beam might produce damage artifacts that might have contributed uncertainty to the interpretation of the images. However, no damage from the x-ray beam was observed in our samples. Only a few gas filled conduits were found at high water potentials in two species, which was to be expected given our sampling design, i.e., excising small shoots in air, as a small portion of conduits originating in the stem would extend into the leaf (Scoffoni and Sack, 2015). Another indication that the microCT faithfully represents mesophyll structure is that cell dimensions measured in the microCT scan images for hydrated leaves were statistically similar to those made on fully hydrated leaves of the same species using light microscopy (repeated measures ANOVA were performed in Minitab 16; results in Table S3).

Measuring leaf and leaf xylem hydraulic vulnerability curves

Leaf hydraulic vulnerability curves for seven of the eight study species were previously published for the same individuals used in this study (Scoffoni et al., 2011; Scoffoni and Sack, 2015), and that for *Malosma laurina* was constructed for this study. Measurements of K_{leaf} vulnerability were made using the evaporative flux method (EFM; see Supplementary Material and Methods; Sack et al., 2002; Scoffoni et al., 2012), for which detailed protocols are available (Sack and Scoffoni, 2012). All measurements were performed on leaves acclimated to high light for over 30 min ($>1000 \mu\text{mol photons m}^{-2} \text{s}^{-1}$). We constructed K_x vulnerability curves using the vacuum pump method (see Supplementary Material and Methods) for the same individuals and species than those from which K_{leaf} vulnerability curves were obtained. Data for four species were previously published in a study of potential methodological artifacts in leaf hydraulic measurements (i.e., *Comarostaphylis diversifolia*, *Hedera canariensis*, *Quercus agrifolia* and *Salvia canariensis*; Scoffoni and Sack, 2015), and additional measurements were made here for four other species (*Cercocarpus betuloides*, *Lantana camara*, *Magnolia grandiflora* and *Malosma laurina*).

To construct hydraulic vulnerability curves, we selected the maximum likelihood function that best fitted data for each species using the *optim* function in R 3.1.0 (<http://www.r->

project.org; Burnham and Anderson, 2004; Scoffoni et al., 2012). Five functions were tested according to previous studies (Pammenter and Vander Willigen, 1998; Scoffoni et al., 2012): a linear function ($K_z = a\Psi_z + b$), a two parameter sigmoidal function ($K_z = \frac{100}{1 + e^{(a(\Psi_z - b))}}$), a three parameter sigmoidal function ($K_z = \frac{a}{1 + e^{-\frac{\Psi_z - x_0}{b}}}$), a logistic function ($K_z = \frac{a}{1 + (\frac{\Psi_z}{x_0})^b}$), an exponential function ($K_z = y_0 + ae^{-b\Psi_z}$). The K_z and Ψ_z in the above functions represent either the K_{leaf} or K_x and water potentials. Functions were compared using the Akaike Information Criterion (AIC), corrected for low n . The function with the lowest AIC value (differences of >2 considered) was chosen as the maximum likelihood function.

Determination of leaf outside-xylem vulnerability curves

Based on eqn 1 we constructed K_{ox} vulnerability curves from K_{leaf} and K_x values along the water potential range tested for given species, i.e., from maximum K_{leaf} until it had declined to a negligible level. Thus, for the different water potentials, each K_{ox} point was obtained as the reciprocal of the difference between K_{leaf}^{-1} and K_x^{-1} following eqn 1. Please see Supplementary Material and Methods for background and justification of this subtraction method.

Whole plant hydraulic model simulations

We modelled the influence of leaf hydraulic declines on the plant hydraulic system under simulated soil and atmospheric drought using a previously described approach (Osborne and Sack, 2012). The plant hydraulic stomatal model (PHS model) is based on Darcy's law, and assumes steady state flow, and simultaneously resolves water potentials and hydraulic conductance for each plant component, given inputs of soil water potential and vapor pressure deficit (VPD) and parameters for the response of the hydraulic conductance of whole root, whole stem, leaf xylem and outside xylem, and stomatal conductance (g_s) to water potential within the respective organ. For the four species tested, we simulated the impact of declining soil water potential or increasing VPD given the measured vulnerability curves for K_{ox} and K_x , obtained as described above. We did not have data for the response of the stem, root or stomata to dehydration for these species, so we used estimates based on current understanding in the literature. Thus, we assumed the vulnerability curve of the whole-stem xylem to follow a sigmoid pattern, with maximum hydraulic conductance representing half of the whole plant

resistance (Tyree and Zimmermann, 2002). To be conservative, we assigned to the stem a water potential at 50% loss of hydraulic conductance equal to that of the leaf xylem, since xylem conduits in the stem are expected to undergo air-seeding at similar or more negative water potentials (Tyree and Ewers, 1991; Choat et al., 2005). Thus, the stem xylem was modelled as potentially more sensitive as it might be in reality, making more robust our finding of its low hydraulic decline when the whole plant is droughted, due to the role of leaf hydraulic decline in minimizing tensions in the stem. We assumed the root vulnerability curve to be equal to that of the whole leaf hydraulic vulnerability curve (obtained as described above) given that on average the root and leaf contribute approximately the same resistance throughout the whole plant (Tyree and Zimmermann, 2002), and have both xylem and extra-xylem pathways for water movement (Tyree and Zimmermann, 2002). We set the g_s decline with leaf water potential as similar to that of the vulnerability of the leaf outside-xylem pathways, using a maximum g_s value of 300 mmol m⁻² s⁻¹ across species. A range of alternative parameterizations did not change the overall findings (data not shown). We note that future work will enable more precise calibration of the model, e.g., with vulnerability functions for all organs. Simulations were run in Python 2.7.10 using the “future”, “scipy” and “pandas” packages. Model code is available on request.

Modelling the outside-xylem flow pathways with dehydration

We used a spatially explicit model of outside-xylem flow pathways in the leaf (MOFLO; Buckley et al., 2015) which can be parameterized with leaf anatomy to investigate potential causes of the strong declines in K_{ox} observed with dehydration. We first simulated the impact of anatomical changes alone, based on anatomical measurements at different water potentials, including epidermal, spongy and palisade mesophyll cell shrinkage (obtained from micro-CT images as described above; Figure 5), percent leaf area shrinkage (which influences vein length per leaf area) and percent intercellular airspace change (previously published for these same species and individuals; Scoffoni et al., 2014). Since bundle sheath cell area could not be determined in the micro-CT images, we assumed these cells shrank by the same percentage as spongy mesophyll cells. We then simulated the impact on K_{ox} of decline in membrane permeability, cell connectivity and cell wall thickness at turgor loss point, using values for tissue dimensions observed at turgor loss point. Given that we did not have measurements of membrane permeability, cell connectivity and cell wall thickness at turgor loss point, we

estimated the reduction in these parameters required to cause the observed decline in K_{ox} at turgor loss point. We repeated all of these simulations under two scenarios: with and without an apoplastic barrier at the bundle sheath cells.

Measurement of turgor loss point

Leaf turgor loss point for 7 of 8 species was obtained from pressure-volume curves of previously published studies (Scoffoni et al., 2012; Scoffoni et al., 2014) that were based on the same individuals of the study species. Pressure-volume curves were obtained for five leaves of three individuals of *Malosma laurina* in the fall of 2014 using a detailed published standard protocol (Sack and PrometheusWiki, 2010).

Light microscopy of cells and tissues within leaves

For measurements of leaf cross sectional anatomy, we used images from a previously published study of different anatomical traits made on the same individuals of four study species (John et al., 2013). Briefly, from each leaf center, a 1×0.5 cm rectangle was cut and embedded gradually in low-viscosity acrylic resin (L.R. White; London Resin Company, England) in ethanol, under vacuum over the course of a week, then dried at 55°C overnight. Samples were then sectioned using glass knives (cut using a LKB 7800 KnifeMaker; LKB Produkter; Bromma, Sweden), at 1 μ m thickness in a rotary microtome (Leica Ultracut E, Reichert-Jung, Ca, USA). Sections were stained in 0.01% toluidine blue in 1% sodium borate and imaged using a 5, 10, 20 and 40 \times objective using a light microscope (Leica Lietz DMRB; Leica Microsystems) with camera utilizing SPOT advanced imaging software (SPOT Imaging Solutions; Diagnostic Instruments Inc.; Sterling Heights, MI) for a total image magnification of 287 \times to 2300 \times . Using ImageJ, we measured the vascular bundle area in the midrib, and counted the total number of xylem conduits.

Statistics

To test the causal influences of xylem and outside-xylem conductance decline on whole leaf hydraulic decline we used three analyses. First, we calculated causal effects within species by partitioning changes in leaf resistance ($R_{leaf} = 1/K_{leaf}$) into changes in xylem resistance ($R_x = 1/K_x$) and outside-xylem resistance ($R_{ox} = 1/K_{ox}$); since $R_{leaf} = R_x + R_{ox}$, $\Delta R_{leaf} = \Delta R_x + \Delta R_{ox}$, where Δ

denotes a change between full turgor and either the turgor loss point or P_{50} . Thus, for example, the percent of leaf hydraulic decline due to outside-xylem pathways was calculated as $\Delta R_{ox}/\Delta R_{leaf} \times 100\%$. Then, we estimated the importance of K_x and K_{ox} decline in explaining species-differences in leaf hydraulic vulnerability, i.e., in the water potential at which the leaf lost 50% of its hydraulic conductance ($P_{50,Kleaf}$). We tested whether $P_{50,Kleaf}$ was best predicted by the water potential at 50% decline in xylem hydraulic conductance ($P_{50,Kx}$) or that of outside-xylem hydraulic conductance ($P_{50,Kox}$), or their combined effect, according to the following models: $P_{50,Kleaf} = a + bP_{50,Kx}$, $P_{50,Kleaf} = a + bP_{50,Kox}$, or $P_{50,Kleaf} = a + bP_{50,Kox} + cP_{50,Kx}$. We used maximum likelihood selection of the best model using the *optim* function in R 3.1.0 (Burnham and Anderson, 2004; Scoffoni et al., 2012). The model with the lowest Akaike Information Criterion corrected for low n (AICc) by at least 2 was selected as the maximum likelihood model. We also applied independent effects analysis, which is suited to robustly determine the contribution of correlated predictor variables to an output variable (Murray and Conner, 2009), and thereby calculated the percent contribution of $P_{50,Kx}$ and $P_{50,Kox}$ to the variation across species in $P_{50,Kleaf}$, using the *hier.part* function in R.3.1.0.

Acknowledgments: We thank the Advanced Light Source in Berkeley, California (Beamline 8.3.2), Dula Parkinson for technical assistance, and Steven Jansen for helpful discussion and comments on the manuscript. This work was supported by the US National Science Foundation (Awards #1146514 and 1457279), the Australian Research Council (DP150103863 and LP130101183), USDA-ARS Current Research Information System-5306 21220-004-00, CAPES/Brazil, and grants from NIFA Specialty Crops Research Initiative and from the American Vineyard Foundation. The Advanced Light Source is supported by the Director, Office of Science, Office of Basic Energy Sciences, of the U.S. Department of Energy under Contract No. DE-AC02-05CH11231.

References

- Anderegg WRL, Flint A, Huang C-y, Flint L, Berry JA, Davis FW, Sperry JS, Field CB (2015) Tree mortality predicted from drought-induced vascular damage. *Nature Geoscience* 8: 367-371
- Bartlett MK, Klein T, Jansen S, Choat B, L. S (2016) The correlations and sequence of plant stomatal, hydraulic, and wilting responses to drought. *Proceedings of the National Academy of Sciences of the United States of America* 113: 13098-13103
- Bartlett MK, Scoffoni C, Sack L (2012) The determinants of leaf turgor loss point and prediction of drought tolerance of species and biomes: a global meta-analysis. *Ecology Letters* 15: 393-405
- Blackman CJ, Brodribb TJ, Jordan GJ (2010) Leaf hydraulic vulnerability is related to conduit dimensions and drought resistance across a diverse range of woody angiosperms. *New Phytologist* 188: 1113-1123
- Blackman CJ, Gleason SM, Chang Y, Cook AM, Laws C, Westoby M (2014) Leaf hydraulic vulnerability to drought is linked to site water availability across a broad range of species and climates. *Annals of Botany* 114: 435-440
- Bouche PS, Delzon S, Choat B, Badel E, Brodribb T, Burlett R, Cochard H, Charra-Vaskou K, Lavigne B, Shan L, Mayr S, Morris H, Torres-Ruiz JM, Zufferey V, Jansen S (2016) Are needles of *Pinus pinaster* more vulnerable to xylem embolism than branches? New insights from X-ray computed tomography. *Plant, Cell & Environment* 39: 860-870
- Boyer JS (1985) Water transport. In WR Briggs, ed, *Annual review of plant physiology*, Vol 36, Annual reviews Inc: Palo Alto, CA, USA, pp 473-516
- Brodribb T, Skelton RP, McAdam SAM, Bieniaime D, Lucani CJ, Marmottant P (2016a) Visual quantification of embolism reveals leaf vulnerability to hydraulic failure. *New Phytologist* doi: 10.1111/nph.13846
- Brodribb TJ, Bieniaime D, Marmottant P (2016b) Revealing catastrophic failure of leaf networks under stress. *Proceedings of the National Academy of Sciences of the United States of America* 113: 4865-4869
- Brodribb TJ, Hill RS (2000) Increases in water potential gradient reduce xylem conductivity in whole plants. Evidence from a low-pressure conductivity method. *Plant Physiology* 123: 1021-1027
- Brodribb TJ, Holbrook NM (2003) Stomatal closure during leaf dehydration, correlation with other leaf physiological traits. *Plant Physiology* 132: 2166-2173
- Brodribb TJ, Holbrook NM (2005) Water stress deforms tracheids peripheral to the leaf vein of a tropical conifer. *Plant Physiology* 137: 1139-1146
- Brodribb TJ, Holbrook NM (2006) Declining hydraulic efficiency as transpiring leaves desiccate: two types of response. *Plant Cell and Environment* 29: 2205-2215
- Brodribb TJ, McAdam SAM (2013) Abscissic Acid Mediates a Divergence in the Drought Response of Two Conifers. *Plant Physiology* 162: 1370-1377
- Bucci SJ, Scholz FG, Goldstein G, Meinzer FC, Sternberg LDL (2003) Dynamic changes in hydraulic conductivity in petioles of two savanna tree species: factors and mechanisms contributing to the refilling of embolized vessels. *Plant Cell and Environment* 26: 1633-1645
- Buckley TN (2015) The contributions of apoplastic, symplastic and gas phase pathways for water transport outside the bundle sheath in leaves. *Plant Cell and Environment* 38: 7-22
- Buckley TN, John GP, Scoffoni C, Sack L (2015) How Does Leaf Anatomy Influence Water Transport outside the Xylem? *Plant Physiology* 168: 1616-1635
- Burnham KP, Anderson DR (2004) Multimodel inference - understanding AIC and BIC in model selection. *Sociological Methods & Research* 33: 261-304

- Canny MJ (1986) Water pathways in Wheat leaves. 3. The passage of the mestome sheath and the function of the suberized lamellae. *Physiologia Plantarum* 66: 637-647
- Canny MJ (1988) Water pathways in Wheat leaves. 4. The interpretation of images of a fluorescent apoplastic tracer. *Australian Journal of Plant Physiology* 15: 541-555
- Charra-Vaskou K, Badel E, Burlett R, Cochard H, Delzon S, Mayr S (2012) Hydraulic efficiency and safety of vascular and non-vascular components in *Pinus pinaster* leaves. *Tree Physiology* 32: 1161-1170
- Chaumont F, Tyerman SD (2014) Aquaporins: Highly Regulated Channels Controlling Plant Water Relations. *Plant Physiology* 164: 1600-1618
- Choat B, Jansen S, Brodribb TJ, Cochard H, Delzon S, Bhaskar R, Bucci SJ, Feild TS, Gleason SM, Hacke UG, Jacobsen AL, Lens F, Maherali H, Martinez-Vilalta J, Mayr S, Mencuccini M, Mitchell PJ, Nardini A, Pittermann J, Pratt RB, Sperry JS, Westoby M, Wright IJ, Zanne AE (2012) Global convergence in the vulnerability of forests to drought. *Nature* 491: 752-+
- Choat B, Lahr EC, Melcher P, Zwieniecki MA, Holbrook NM (2005) The spatial pattern of air seeding thresholds in mature sugar maple trees. *Plant, Cell & Environment* 28: 1082-1089
- Cochard H, Badel E, Herbette S, Delzon S, Choat B, Jansen S (2013) Methods for measuring plant vulnerability to cavitation: a critical review. *Journal of Experimental Botany* 64: 4779-4791
- Cochard H, Bodet C, Ameglio T, Cruiziat P (2000) Cryo-scanning electron microscopy observations of vessel content during transpiration in walnut petioles. Facts or artifacts? *Plant Physiology* 124: 1191-1202
- Cochard H, Venisse JS, Barigah TS, Brunel N, Herbette S, Guilliot A, Tyree MT, Sakr S (2007) Putative role of aquaporins in variable hydraulic conductance of leaves in response to light. *Plant Physiology* 143: 122-133
- Coomes DA, S. H, E.R. G, J.J. S, Sack L (2008) Scaling of xylem vessels and veins within the leaves of oak species. *Biology Letters* 4: 302-306
- Crombie DS, Milburn JA, Hipkins MF (1985) Maximum sustainable xylem sap tensions in *Rhododendron* and other species. *Planta* 163: 27-33
- Cuneo IF, Knipfer T, Brodersen C, McElrone AJ (2016) Mechanical failure of fine root cortical cells initiates plant hydraulic decline during drought. *Plant Physiology* doi:10.1104/pp.16.00923
- Diffenbaugh NS, Swain DL, Touma D (2015) Anthropogenic warming has increased drought risk in California. *Proceedings of the National Academy of Sciences of the United States of America* 112: 3931-3936
- Dixon HH, Joly J (1895) On the ascent of sap. *Philosophical Transactions of the Royal Society of London* 186: 563-576
- Guyot G, Scoffoni C, Sack L (2012) Combined impacts of irradiance and dehydration on leaf hydraulic conductance: insights into vulnerability and stomatal control. *Plant, Cell & Environment* 35: 857-871
- Hacke UG, Sperry JS, Pittermann J (2000) Drought experience and cavitation resistance in six shrubs from the Great Basin, Utah. *Basic and Applied Ecology* 1: 31-41
- Hernandez-Santana V, Rodriguez-Dominguez CM, Fernández JE, Diaz-Espejo A (2016) Role of leaf hydraulic conductance in the regulation of stomatal conductance in almond and olive in response to water stress. *Tree Physiology* 00: 1-11
- Hochberg U, Albuquerque C, Rachmilevitch S, Cochard H, David-Schwartz R, Brodersen CR, McElrone A, Windt CW (2016) Grapevine petioles are more sensitive to drought induced embolism than stems: evidence from in vivo MRI and microcomputed tomography observations of hydraulic vulnerability segmentation. *Plant, Cell & Environment*: n/a-n/a

- 658 Johansson I, Karlsson M, Shukla VK, Chrispeels MJ, Larsson C, Kjellbom P (1998) Water transport
659 activity of the plasma membrane aquaporin PM28A is regulated by phosphorylation. *Plant*
660 *Cell* 10: 451-459
- 661 John GP, Scoffoni C, Sack L (2013) Allometry of cells and tissues within leaves. *American Journal of*
662 *Botany*: 100: 1936-1948
- 663 Johnson DM, McCulloh KA, Woodruff DR, Meinzer FC (2012) Evidence for xylem embolism as a
664 primary factor in dehydration-induced declines in leaf hydraulic conductance. *Plant Cell and*
665 *Environment* 35: 760-769
- 666 Johnson DM, Meinzer FC, Woodruff DR, McCulloh KA (2009a) Leaf xylem embolism, detected
667 acoustically and by cryo-SEM, corresponds to decreases in leaf hydraulic conductance in four
668 evergreen species. *Plant Cell and Environment* 32: 828-836
- 669 Johnson DM, Woodruff DR, McCulloh KA, Meinzer FC (2009b) Leaf hydraulic conductance, measured
670 in situ, declines and recovers daily: leaf hydraulics, water potential and stomatal conductance
671 in four temperate and three tropical tree species. *Tree Physiology* 29: 879-887
- 672 Kikuta SB, LoGullo MA, Nardini A, Richter H, Salleo S (1997) Ultrasound acoustic emissions from
673 dehydrating leaves of deciduous and evergreen trees. *Plant Cell and Environment* 20: 1381-
674 1390
- 675 Kim YX, Steudle E (2007) Light and turgor affect the water permeability (aquaporins) of parenchyma
676 cells in the midrib of leaves of *Zea mays*. *Journal of Experimental Botany* 58: 4119-4129
- 677 Kim YX, Steudle E (2009) Gating of aquaporins by light and reactive oxygen species in leaf parenchyma
678 cells of the midrib of *Zea mays*. *Journal of Experimental Botany* 60: 547-556
- 679 Knipfer T, Cuneo IF, Brodersen CR, McElrone AJ (2016) In situ visualization of the dynamics in xylem
680 embolism formation and removal in the absence of root pressure: a study on excised
681 grapevine stems. *Plant Physiology* 171: 1024-1036
- 682 Laur J, Hacke UG (2014) Exploring *Picea glauca* aquaporins in the context of needle water uptake and
683 xylem refilling. *New Phytologist* 203: 388-400
- 684 Lersten NR (1997) Occurrence of endodermis with a casparian strip in stem and leaf. *Botanical Review*
685 63: 265-272
- 686 Lo Gullo MA, Nardini A, Trifilo P, Salleo S (2003) Changes in leaf hydraulics and stomatal conductance
687 following drought stress and irrigation in *Ceratonia siliqua* (Carob tree). *Physiologia Plantarum*
688 117: 186-194
- 689 Maurel C, Boursiac Y, Luu D-T, Santoni V, Shahzad Z, Verdoucq L (2015) Aquaporins in Plants.
690 *Physiological reviews* 95: 1321-1358
- 691 McAdam SAM, Brodribb TJ (2014) Separating Active and Passive Influences on Stomatal Control of
692 Transpiration. *Plant Physiology* 164: 1578-1586
- 693 McKown Athena D, Cochard H, Sack L (2010) Decoding leaf hydraulics with a spatially explicit model:
694 principles of venation architecture and implications for its evolution. *The American Naturalist*
695 175: 447-460
- 696 Milburn JA (1966) Conduction of sap. I. Water conduction and cavitation in water stressed leaves.
697 *Planta* 69: 34-&
- 698 Milburn JA, Johnson RPC (1966) Conductance of sap. 2. Detection of vibrations produced by sap
699 cavitation in *Ricinus* xylem. *Planta* 69: 43-52
- 700 Miyazawa S, Yoshimura S, Shinzaki Y, Maeshima M, Miyake C (2008) Deactivation of aquaporins
701 decreases internal conductance to CO₂ diffusion in tobacco leaves grown under long-term
702 drought. *Functional Plant Biology* 35: 553-564

- Moshelion M, Halperin O, Wallach R, Oren R, Way DA (2015) Role of aquaporins in determining transpiration and photosynthesis in water-stressed plants: crop water-use efficiency, growth and yield. *Plant Cell and Environment* 38: 1785-1793
- Murray K, Conner MM (2009) Methods to quantify variable importance: implications for the analysis of noisy ecological data *Ecology* 90: 348-355
- Nardini A, Ramani M, Gortan E, Salleo S (2008) Vein recovery from embolism occurs under negative pressure in leaves of sunflower (*Helianthus annuus*). *Physiologia Plantarum* 133: 755-764
- Nardini A, Salleo S (2000) Limitation of stomatal conductance by hydraulic traits: sensing or preventing xylem cavitation? *Trees-Structure and Function* 15: 14-24
- Nardini A, Salleo S (2003) Effects of the experimental blockage of the major veins on hydraulics and gas exchange of *Prunus laurocerasus* L. leaves. *Journal of Experimental Botany* 54: 1213-1219
- Nardini A, Salleo S, Raimondo F (2003) Changes in leaf hydraulic conductance correlate with leaf vein embolism in *Cercis siliquastrum* L. *Trees-Structure and Function* 17: 529-534
- Nardini A, Tyree MT, Salleo S (2001) Xylem cavitation in the leaf of *Prunus laurocerasus* and its impact on leaf hydraulics. *Plant Physiology* 125: 1700-1709
- North GB, Martre P, Nobel PS (2004) Aquaporins account for variations in hydraulic conductance for metabolically active root regions of *Agave deserti* in wet, dry, and rewetted soil. *Plant Cell and Environment* 27: 219-228
- Osborne CP, Sack L (2012) Evolution of C-4 plants: a new hypothesis for an interaction of CO₂ and water relations mediated by plant hydraulics. *Philosophical Transactions of the Royal Society B-Biological Sciences* 367: 583-600
- Pammenter NW, Vander Willigen C (1998) A mathematical and statistical analysis of the curves illustrating vulnerability of xylem to cavitation. *Tree Physiology* 18: 589-593
- Pantin F, Monnet F, Jannaud D, Costa JM, Renaud J, Muller B, Simonneau T, Genty B (2013) The dual effect of abscisic acid on stomata. *New Phytologist* 197: 65-72
- Pierce M, Raschke K (1980) Correlation between loss of turgor and accumulation of abscisic acid in detached leaves. *Planta* 148: 174-182
- Pieruschka R, Huber G, Berry JA (2010) Control of transpiration by radiation. *Proceedings of the National Academy of Sciences of the United States of America* 107: 13372-13377
- Pou A, Medrano H, Flexas J, Tyerman SD (2013) A putative role for TIP and PIP aquaporins in dynamics of leaf hydraulic and stomatal conductances in grapevine under water stress and re-watering. *Plant Cell and Environment* 36: 828-843
- Prado K, Maurel C (2013) Regulation of leaf hydraulics: from molecular to whole plant levels. *Frontiers in plant science* 4
- Ribeiro MLRC, Santos MG, Moraes MG (2007) Leaf anatomy of two *Anemia* Sw. species (Schizaeaceae-Pteridophyte) from a rocky outcrop in Niteroi, Rio de Janeiro, Brazil. *Revista Brasileira de Botanica* 30: 695-702
- Ritman KT, Milburn JA (1988) Acoustic emissions from plants- Ultrasonic and audible compared. *Journal of Experimental Botany* 39: 1237-1248
- Rockwell FE, Holbrook NM, Stroock AD (2014) The Competition between Liquid and Vapor Transport in Transpiring Leaves. *Plant Physiology* 164: 1741-1758
- Sack L, Ball MC, Brodersen C, Donovan L, Givnish TJ, Hacke U, Huxman TE, Jacobsen AL, Jansen S, Johnson DM, G. K, Lachenbruch B, Maurel C, McCulloch KA, McDowell N, McElrone AJ, Meinzer F, Melcher P, North GB, Pellegrini M, Pockman WT, Pratt RB, Rockwell FE, Sala A, Santiago LS, Scoffoni C, Sevanto SA, Sperry J, Spicer RA, Davies SJ, Tyerman SD, Way DA, Zweiniecki MA, Holbrook MN (2016a) Plant water transport as a central hub from plant to

- ecosystem function: meeting report for “Emerging Frontiers in Plant Hydraulics” (Washington, DC, May 2015). *Plant, Cell & Environment*: In Press.
- Sack L, Buckley TN, Scoffoni C (2016b) Why are leaves hydraulically vulnerable? *Journal of Experimental Botany* 67: 4917-4919
- Sack L, Holbrook NM (2006) Leaf hydraulics. *Annual Review of Plant Biology* 57: 361-381
- Sack L, Melcher PJ, Zwieniecki MA, Holbrook NM (2002) The hydraulic conductance of the angiosperm leaf lamina: a comparison of three measurement methods. *Journal of Experimental Botany* 53: 2177-2184
- Sack L, PrometheusWiki (2010) Leaf pressure-volume curve parameters *In*. PrometheusWiki [http://www.publish.csiro.au/prometheuswiki/tiki-pagehistory.php?page=Leaf pressure-volume curve parameters&preview=10](http://www.publish.csiro.au/prometheuswiki/tiki-pagehistory.php?page=Leaf%20pressure-volume%20curve%20parameters&preview=10)
- Sack L, Scoffoni C (2012) Measurement of leaf hydraulic conductance and stomatal conductance and their responses to irradiance and dehydration using the evaporative flux methods (EFM). *Journal of Visualized Experiments* e4179: 1-7
- Sack L, Scoffoni C (2013) Leaf venation: structure, function, development, evolution, ecology and applications in past, present and future. *New Phytologist* 198: 938-1000
- Sack L, Streeter CM, Holbrook NM (2004) Hydraulic analysis of water flow through leaves of sugar maple and red oak. *Plant Physiology* 134: 1824-1833
- Sade N, Shatil-Cohen A, Attia Z, Maurel C, Boursiac Y, Kelly G, Granot D, Yaaran A, Lerner S, Moshelion M (2014) The Role of Plasma Membrane Aquaporins in Regulating the Bundle Sheath-Mesophyll Continuum and Leaf Hydraulics. *Plant Physiology* 166: 1609-+
- Sade N, Shatil-Cohen A, Moshelion M (2015) Bundle-sheath aquaporins play a role in controlling *Arabidopsis* leaf hydraulic conductivity. *Plant Signaling & Behavior* 10
- Salleo S, Lo Gullo MA, Raimondo F, Nardini A (2001) Vulnerability to cavitation of leaf minor veins: any impact on leaf gas exchange? *Plant Cell and Environment* 24: 851-859
- Salleo S, Nardini A, Pitt F, Lo Gullo MA (2000) Xylem cavitation and hydraulic control of stomatal conductance in Laurel (*Laurus nobilis* L.). *Plant Cell and Environment* 23: 71-79
- Sancho-Knapik D, Alvarez-Arenas TG, Peguero-Pina JJ, Fernandez V, Gil-Pelegrin E (2011) Relationship between ultrasonic properties and structural changes in the mesophyll during leaf dehydration. *Journal of Experimental Botany* 62: 3637-3645
- Sandford AP, Grace J (1985) The measurement and interpretation of ultrasound from woody stems. *Journal of Experimental Botany* 36: 298-311
- Scoffoni C, Albuquerque C, Brodersen CR, Townes ST, John GP, Cochard H, Buckley TN, McElrone AJ, L. S (2016) Leaf vein xylem conduit diameter influences susceptibility to embolism and hydraulic decline. *New Phytologist*: doi:10.1111/nph.14256
- Scoffoni C, McKown AD, Rawls M, Sack L (2012) Dynamics of leaf hydraulic conductance with water status: quantification and analysis of species differences under steady-state. *Journal of Experimental Botany* 63: 643-658
- Scoffoni C, Pou A, Aasamaa K, Sack L (2008) The rapid light response of leaf hydraulic conductance: new evidence from two experimental methods. *Plant Cell and Environment* 31: 1803-1812
- Scoffoni C, Rawls M, McKown A, Cochard H, Sack L (2011) Decline of leaf hydraulic conductance with dehydration: relationship to leaf size and venation architecture. *Plant Physiology* 156: 832-843
- Scoffoni C, Sack L (2015) Are leaves “freewheelin”? Testing for a Wheeler-type effect in leaf xylem hydraulic decline. *Plant, Cell & Environment* 38: 534-543
- Scoffoni C, Vuong C, Diep S, Cochard H, Sack L (2014) Leaf shrinkage with dehydration: coordination with hydraulic vulnerability and drought tolerance. *Plant Physiology* 164: 1772-1788

- 795 Shatil-Cohen A, Attia Z, Moshelion M (2011) Bundle-sheath cell regulation of xylem-mesophyll water
796 transport via aquaporins under drought stress: a target of xylem-borne ABA? *Plant Journal* 67:
797 72-80
- 798 Shatil-Cohen A, Moshelion M (2012) Smart pipes: the bundle sheath role as xylem-mesophyll barrier.
799 *Plant signaling & behavior* 7: 1088-1091
- 800 Sheffield J, Wood EF, Roderick ML (2012) Little change in global drought over the past 60 years.
801 *Nature* 491: 435-+
- 802 Stiller V, Laitte HR, Sperry JS (2003) Hydraulic properties of rice and the response of gas exchange to
803 water stress. *Plant Physiology* 132: 1698-1706
- 804 Taneda H, Raj Kandel D, Ishida A, Ikeda H (2016) Altitudinal changes in leaf hydraulic conductance
805 across five *Rhododendron* species in eastern Nepal. *Tree Physiology* In Press
- 806 Taneda H, Terashima I (2012) Co-ordinated development of the leaf midrib xylem with the lamina in
807 *Nicotiana tabacum*. *Annals of Botany* 110: 35-45
- 808 Trifilo P, Gasco A, Raimondo F, Nardini A, Salleo S (2003a) Kinetics of recovery of leaf hydraulic
809 conductance and vein functionality from cavitation-induced embolism in sunflower. *Journal of*
810 *Experimental Botany* 54: 2323-2330
- 811 Trifilo P, Nardini A, Lo Gullo MA, Salleo S (2003b) Vein cavitation and stomatal behaviour of sunflower
812 (*Helianthus annuus*) leaves under water limitation. *Physiologia Plantarum* 119: 409-417
- 813 Trifilo P, Raimondo F, Savi T, Lo Gullo MA, Nardini A (2016) The contribution of vascular and extra-
814 vascular water pathways to drought-induced decline of leaf hydraulic conductance. *Journal of*
815 *Experimental Botany* In Press
- 816 Tyree MT, Ewers FW (1991) The hydraulic architecture of trees and other woody-plants. *New*
817 *Phytologist* 119: 345-360
- 818 Tyree MT, Sperry JS (1989) Vulnerability of xylem to cavitation and embolism. *Annual Review of Plant*
819 *Physiology and Plant Molecular Biology* 40: 19-38
- 820 Tyree MT, Yianoulis P (1980) The site of water evaporation from sub-stomatal cavities, liquid path
821 resistances and hydroactive stomatal closure. *Annals of Botany* 46: 175-193
- 822 Tyree MT, Zimmermann MH (2002) *Xylem Structure and the Ascent of Sap*. Springer, Berlin, Germany.
- 823 Urli M, Porte AJ, Cochard H, Guengant Y, Burlett R, Delzon S (2013) Xylem embolism threshold for
824 catastrophic hydraulic failure in angiosperm trees. *Tree Physiology* 33: 672-683
- 825 Vandeleur RK, Sullivan W, Athman A, Jordans C, Gilliam M, Kaiser BN, Tyerman SD (2014) Rapid
826 shoot-to-root signalling regulates root hydraulic conductance via aquaporins. *Plant Cell and*
827 *Environment* 37: 520-538
- 828 Vicente-Serrano SM, Lopez-Moreno JJ, Begueria S, Lorenzo-Lacruz J, Sanchez-Lorenzo A, Garcia-Ruiz
829 JM, Azorin-Molina C, Moran-Tejeda E, Revuelto J, Trigo R, Coelho F, Espejo F (2014) Evidence
830 of increasing drought severity caused by temperature rise in southern Europe. *Environmental*
831 *Research Letters* 9
- 832 Wan XC, Steudle E, Hartung W (2004) Gating of water channels (aquaporins) in cortical cells of young
833 corn roots by mechanical stimuli (pressure pulses): effects of ABA and of HgCl₂. *Journal of*
834 *Experimental Botany* 55: 411-422
- 835 Woodruff DR, McCulloh KA, Warren JM, Meinzer FC, Lachenbruch B (2007) Impacts of tree height on
836 leaf hydraulic architecture and stomatal control in Douglas-fir. *Plant Cell and Environment* 30:
837 559-569
- 838 Wu XQ, Lin JX, Lin QQ, Wang J, Schreiber L (2005) Casparian strips in needles are more solute
839 permeable than endodermal transport barriers in roots of *Pinus bungeana*. *Plant and Cell*
840 *Physiology* 46: 1799-1808

- 841 **Wylie RB (1947) Conduction in dicotyledon leaves The Proceedings of the Iowa Academy of Science**
842 **53: 195—202**
- 843 **Ye Q, Muhr J, Steudle E (2005) A cohesion/tension model for the gating of aquaporins allows**
844 **estimation of water channel pore volumes in Chara. Plant Cell and Environment 28: 525-535**
- 845 **Zhang YJ, Rockwell FE, Graham AC, Holbrook MN (2016) Reversible leaf xylem collapse: a potential**
846 **'circuit breaker' against cavitation. Plant Physiology doi:10.1104/pp.16.01191**

847

848

849 Figure Captions

850 **Figure 1.** Leaf hydraulic conductance (K_{leaf}) characterizes the water transport capacity of the
 851 whole leaf, and is influenced by (A) water movement through the leaf xylem (K_x), and (B)
 852 through the mesophyll, or outside-xylem pathways (K_{ox}), which includes vascular parenchyma,
 853 bundle sheath, and mesophyll cell pathways for liquid and/or vapor phase transport and diffusion
 854 through airspaces (red dots) through stomata. As the leaf dehydrates, observed declines in K_{leaf}
 855 have typically been primarily attributed to reduction of K_x due to the formation of embolism in
 856 xylem conduits, though recent studies suggested a possible role for changes in outside-xylem
 857 pathways properties via reduced membrane permeability and cell shrinkage. Symbols: xylem
 858 (X), bundle sheath cell (BS), spongy mesophyll cell (SM), palisade mesophyll cell (PM), upper
 859 epidermal cell (UE), lower epidermal cell (LE), stomata (S).

860 **Figure 2.** Low vulnerability of the leaf xylem to embolism before turgor loss point as revealed
 861 by *in vivo* imaging of leaves of four diverse angiosperm species subjected to progressive
 862 dehydration (i.e., increasingly negative leaf water potential, Ψ_{leaf}) using X-ray micro-computed
 863 tomography (microCT). (A-L) scans of leaf midribs at mild dehydration, turgor loss point and
 864 extreme dehydration (an illustrative image for each range is shown from left to right), showing
 865 very few embolized midrib conduits above turgor loss point. No emboli were observed in higher
 866 order veins above turgor loss point, and few were observed even in extremely dehydrated leaves
 867 (data not shown). Note that *Comarostaphylis diversifolia* contains embolized protoxylem
 868 conduits, which are hydraulically non-functional, even for well hydrated leaves, and these
 869 protoxylem conduits are included in the calculations of embolized conduits. Scale = 250 μm .

870 **Figure 3.** The vulnerability of whole leaf hydraulic conductance (K_{leaf} ; green) to dehydration is
 871 mainly determined by the vulnerability of the outside-xylem pathways (K_{ox} ; dashed-black), and
 872 not that of the xylem (K_x ; light grey) across the four species for which microCT was performed
 873 (left panels) and an additional expanded set of four diverse species (right panels). The maximum
 874 likelihood function is plotted for each vulnerability curve (*see Methods*). The turgor loss point
 875 for each species is represented by a dotted black line.

876 **Figure 4.** Model simulations of whole plant hydraulic response to (A) atmospheric drought
 877 (increasing vapor pressure deficit, VPD). and (B) dehydrating soil. PLC values plotted in both

panels are averages of simulations obtained for the four species tested (see *Methods*). The percent loss of hydraulic conductance (PLC) outside the xylem (ox; grey solid line) is the main determinant of the decline of whole plant hydraulic conductance (p; black solid line) under both scenarios. Neither leaf xylem hydraulic conductance (x; medium dash light blue line) nor stem xylem hydraulic conductance (s; dotted dark blue line) experience strong declines with increasing soil drought or VPD. The root hydraulic conductance (small dashed red line) declines strongly under increasing soil drought, and to a smaller extent under increasing VPD. Because the model simulates a transpiring plant, when the soil water potential is at zero on the x -axis, the transpiring leaf water potential is still substantially negative, driving the decline of K_{leaf} from its maximum value (though not of K_x ; please see Table S2 for water potentials of each compartment). Under the soil drought scenario, VPD was maintained at 0.5 kPa. Under the atmospheric drought scenario, soil water potential was maintained at -0.1 MPa.

Figure 5. X-ray micro-computed tomography scans of leaf laminas at three dehydration levels for four species. Symbols: Leaf water potential (Ψ_{leaf}), vascular bundle (V), spongy mesophyll cell (S), palisade mesophyll cell (P), upper epidermal cell (UE), lower epidermal cell (LE). Scale = 250 μm .

Figure 6. Testing hypotheses for the potential drivers of the decline in outside-xylem hydraulic conductance in dehydrating leaves, using a spatially explicit model of leaf outside-xylem water transport (see *Methods*). Parameterizing the model for four species, we estimated the outside-xylem hydraulic conductance (K_{ox}) based on the decline of observed cell size, porosity (airspace) and leaf area at turgor loss point (light grey bars). Because in some cases these changes in tissue dimensions resulted in an *increase* in K_{ox} , we modelled K_{ox} decline according to three scenarios (always including the observed changes in tissue dimension): an 80% decline at turgor loss point in membrane permeability (blue bars), cell connectivity (red bars), and cell wall thickness (dark grey bar). All simulations were run with or without including an apoplastic barrier at the bundle sheath cells (filled vs. striped bars). The yellow star on the x -axis represents the observed % K_{ox} decline at turgor loss point. Across all four species, only simulations of a strong decrease in membrane permeability in leaves with an apoplastic barrier could explain the observed declines in K_{ox} .

SUPPLEMENTAL DATA

Figure S1. Decline of leaf xylem hydraulic conductance (K_x) with dehydration.

Figure S2. Model simulations of plant hydraulic response to dehydrating soil (top panels) and increasing vapor pressure deficit (VPD; bottom panels) for four diverse species.

Figure S3. Light-microscopy midrib cross-sections of the four study species used for x-ray micro-computed tomography.

Figure S4. Percent midrib vascular area of maximum at full hydration plotted against leaf water potential.

Table S1. Parameters for the three models tested to best predict the water potential at which leaf hydraulic conductance declined by 50% ($P_{50,K_{leaf}}$).

Table S2 (Excel spreadsheet). Inputs and results for the whole plant hydraulic model simulations.

Table S3. Mean \pm standard errors of cell dimensions measured from x-ray micro-computed tomography scans and light microscopy.

Figure S1. Decline of leaf xylem hydraulic conductance (K_x) with dehydration. The maximum likelihood function is plotted for each vulnerability curve (*see Methods*).

Figure S2. Model simulations of plant hydraulic response to dehydrating soil (top panels) and increasing vapor pressure deficit (VPD; bottom panels) for four diverse species. The percent loss of leaf hydraulic conductance (PLC) outside the xylem (grey solid line) is the main determinant of the decline of whole plant hydraulic conductance (black solid line) in the drought tolerant species under both scenarios. The leaf xylem (K_x ; dotted light blue line) and stem xylem (dotted dark blue line) hydraulic conductance are protected from tensions that would result in strong declines under increasing soil drought or VPD. The root hydraulic conductance also strongly declines (red dotted lines) under increasing soil drought, though not as strongly as that of the leaf

outside-xylem pathways, and much less strongly under increasing VPD. In *Lantana camara*, steep declines in all hydraulic compartments were observed under soil drought simulations, but under increasing VPD, the decline of outside-xylem hydraulic conductance (K_{ox}) is much stronger and protects the other compartments of the plant from high tensions, as for the other species. Notably, because the model is simulating a transpiring plant, when the soil water potential is at zero on the x -axis, the transpiring leaf water potential is still substantially negative, leading to decline of K_{leaf} (though not of K_x ; please see Table S2 for water potentials of each compartment).

Figure S3. Light-microscopy midrib cross-sections of the four study species used for x-ray micro-computed tomography. Scale = 500 μ m

Figure S4. Percent midrib vascular area of maximum at full hydration plotted against leaf water potential. The slope and intercept of each regression were used to estimate the proportion area shrinkage relative to the value extrapolated to 0 MPa (AS_{dehydr}). * $p < 0.05$, ** $p < 0.01$ and *** $p < 0.001$.

Table 1. Study species, family, origin, plant and leaf habit, and mean values \pm standard errors for hydraulic vulnerability traits: water potential at which whole leaf, leaf xylem and leaf outside-xylem hydraulic conductance declined by 50% ($P_{50,K_{leaf}}$, P_{50,K_x} and $P_{50,K_{ox}}$ respectively), and the turgor loss point (Ψ_{TLP}).

Table 2. Percent embolized midrib conduits (%EMC) obtained from microCT imaging, at three water potential intervals. Mean \pm standard errors are given, with the number of sample indicated in parenthesis.

Table 3. Results from the Taylor series multiplicative approximation, testing the causality of K_x and K_{ox} decline on K_{leaf} decline at turgor loss point (TLP) and water potential at which K_{leaf} declined by 50% (P_{50}).

Table S1. Parameters for the three models tested to best predict the water potential at which leaf hydraulic conductance declined by 50% ($P_{50,K_{leaf}}$), as a function of the water potential at which the hydraulic conductance of the xylem and outside xylem pathways declined by 50% (P_{50,K_x} and $P_{50,K_{ox}}$ respectively), r^2 for observed $P_{50,K_{leaf}}$ values plotted against those predicted from the

961 model, and values for the Akaike Information Criterion corrected for low n (AICc). The
962 maximum-likelihood function appears in bold.

963 **Table S2 (Excel spreadsheet).** Inputs and results for the whole plant hydraulic model
964 simulations.

965 **Table S3.** Mean \pm standard errors of cell dimensions measured from x-ray micro-computed
966 tomography scans and light microscopy. Values from micro-CT scans were averaged across
967 leaves of water potentials > -0.50 MPa ($n = 2-5$). Values from light microscopy are from fully
968 hydrated leaves reported by John et al., 2013. P -values shown are results from t -tests between
969 micro-CT and light microscopy cell dimensions values.

Table 1. Study species, family, origin, plant and leaf habit, and mean values \pm standard errors for hydraulic vulnerability traits: water potential at which whole leaf (K_{leaf}), leaf xylem (K_x) and leaf outside-xylem hydraulic conductance (K_{ox}) declined by 50% (P_{50}) and 88% (P_{88}), and the turgor loss point (Ψ_{TLP}).

Species	Family	Origin	Plant habit	Leaf habit	P_{50} and $P_{88, K_{leaf}}$ (MPa)	P_{50} and $P_{88, K_{ox}}$ (MPa)	P_{50} and P_{88, K_x} (MPa)	Ψ_{TLP} (MPa)
<i>Cercocarpus betuloides</i>	Rosaceae	California, Mexico	Tree	Evergreen	-2.8, -6.5	-2.8, -6.2	-3.0, -6.6	-2.6 \pm 0.04
<i>Comarostaphylis diversifolia</i>	Ericaceae	California, Mexico	Tree	Evergreen	-2.8, -5.0	-2.7, -5.0	-5.6, -8.4	-3.4 \pm 0.34
<i>Hedera canariensis</i>	Araliaceae	Canary Islands	Shrub	Evergreen	-0.64, -1.5	-0.58, -1.3	-1.9, -2.8	-2.0 \pm 0.07
<i>Lantana camara</i>	Verbenaceae	Panropical	Shrub	Deciduous	-0.80, -1.8	-0.79, -1.8	-0.87, -1.6	-1.4 \pm 0.04
<i>Magnolia grandiflora</i>	Magnoliaceae	Southern USA	Tree	Evergreen	-0.42, -4.1	-0.33, -2.6	-3.3, -4.6	-2.1 \pm 0.02
<i>Malosma laurina</i>	Anacardiaceae	California, Mexico	Shrub	Evergreen	-0.64, -1.4	-0.35, -0.95	-2.6, -5.2	-2.2 \pm 0.06
<i>Quercus agrifolia</i>	Fagaceae	California, Mexico	Tree	Evergreen	-2.4, -4.2	-2.2, -4.1	-5.4, -6.7	-3.0 \pm 0.12
<i>Salvia canariensis</i>	Lamiaceae	Canary Islands	Shrub	Evergreen	-0.26, -0.76	-0.09, -0.36	-0.89, -1.6	-1.2 \pm 0.05

Table 2. Percent embolized midrib conduits (%EMC) obtained from x-ray computed micro-tomography (microCT) imaging, at three water potential intervals. Mean \pm standard errors are given, with the number of measured leaves indicated in parentheses.

Species	Mild dehydration		Dehydration to turgor loss point		Strong dehydration	
	Water potential (MPa)	% EMC	Water potential (MPa)	% EMC	Water potential (MPa)	% EMC
<i>Comarostaphylis diversifolia</i>	-1.14 \pm 0.56	4.84 \pm 0.69 (5)	-3.37 \pm 0.06	5.68 \pm 0.60 (3)	-7.31 \pm 0.53	5.27 \pm 0.87 (4)
<i>Hedera canariensis</i>	-0.24 \pm 0.04	5.56 \pm 2.25 (5)	-1.61 \pm 0.08	8.51 \pm 2.25 (3)	-3.13 \pm 0.36	19.6 \pm 10.9 (4)
<i>Lantana camara</i>	-0.51 \pm 0.22	6.30 \pm 2.59 (4)	-1.07 \pm 0.01	6.40 \pm 0.13 (2)	-1.34 \pm 0.04	36.8 \pm 15.8 (3)
<i>Magnolia grandiflora</i>	-0.06 \pm 0.006	0.88 \pm 1.83 (3)	-1.35 \pm 0.30	4.96 \pm 2.18 (3)	-5.64 \pm 0.85	43.9 \pm 21.9 (5)

Table 3. Percentages of increase in leaf hydraulic resistance ($1/K_{\text{leaf}}$) contributed by increases in xylem resistance ($1/K_x$) and outside-xylem resistance ($1/K_{\text{ox}}$), at turgor loss point (TLP) and at the water potential at which K_{leaf} declined by 50% (P_{50}) and by 88% (P_{88}).

Species	% Influence on K_{leaf} decline at TLP		% Influence on K_{leaf} decline at leaf P_{50}		% Influence on K_{leaf} decline at leaf P_{88}	
	K_x	K_{ox}	K_x	K_{ox}	K_x	K_{ox}
<i>Cercocarpus betuloides</i>	9.4	90.6	5.1	94.9	8.2	91.8
<i>Comarostaphylis diversifolia</i>	1.1	98.9	1.1	98.9	0.7	99.3
<i>Hedera canariensis</i>	2.2	97.8	0.9	99.1	1.4	98.6
<i>Lantana camara</i>	14.3	85.7	2.9	97.1	24.8	75.2
<i>Magnolia grandiflora</i>	0.7	99.3	0.1	99.9	9.7	90.3
<i>Malosma laurina</i>	0.9	99.1	2.4	97.5	2.9	97.1
<i>Quercus agrifolia</i>	0	100	0	100	0.2	99.8
<i>Salvia canariensis</i>	4.7	95.3	0.7	99.2	8.0	92.0

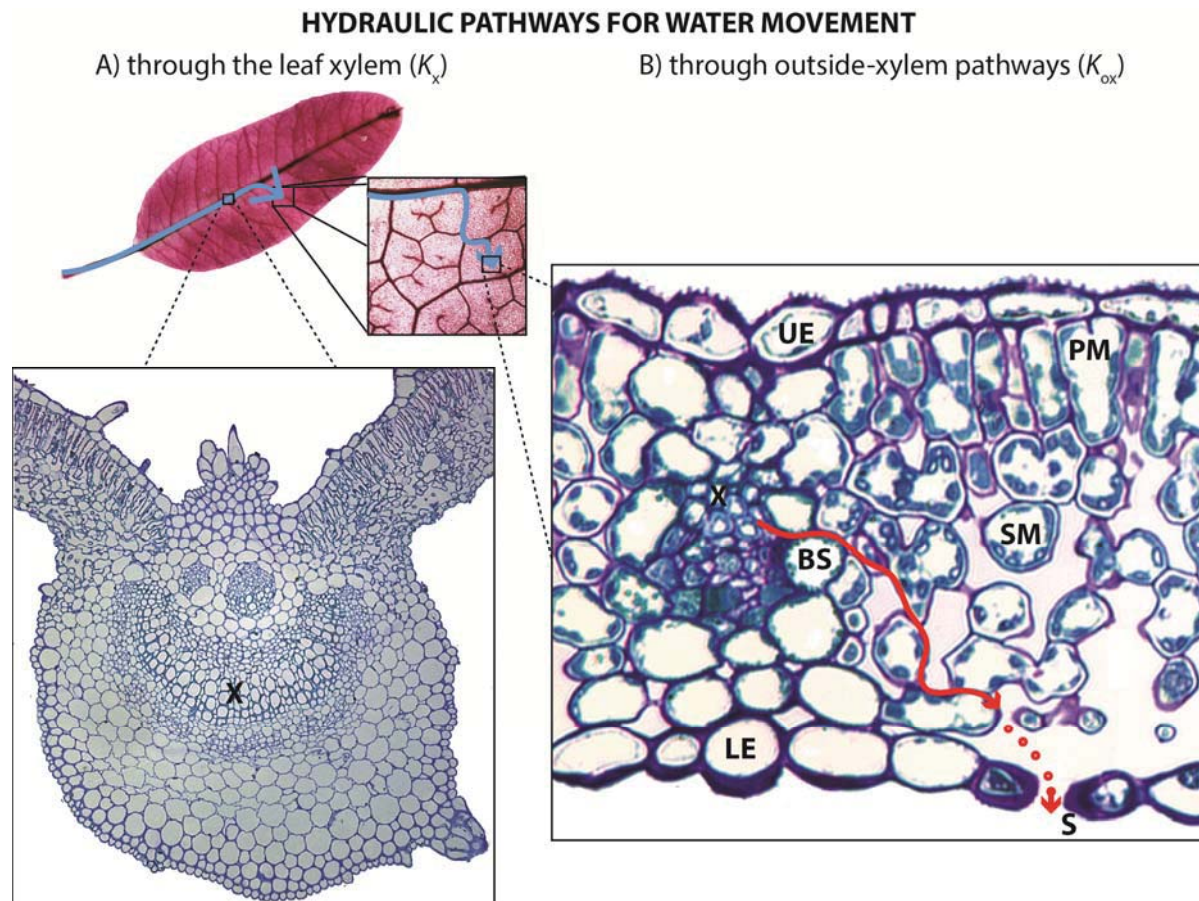


Figure 1

Figure 1. Leaf hydraulic conductance (K_{leaf}) characterizes the water transport capacity of the whole leaf, and is influenced by (A) water movement through the leaf xylem (K_x), and (B) through the mesophyll, or outside-xylem pathways (K_{ox}), which includes vascular parenchyma, bundle sheath, and mesophyll cell pathways for liquid and/or vapor phase transport and diffusion through airspaces (red dots) through stomata. As the leaf dehydrates, observed declines in K_{leaf} have typically been primarily attributed to reduction of K_x due to the formation of embolism in xylem conduits, though recent studies suggested a possible role for changes in outside-xylem pathways properties via reduced membrane permeability and cell shrinkage. Symbols: xylem

(X), bundle sheath cell (BS), spongy mesophyll cell (SM), palisade mesophyll cell (PM), upper epidermal cell (UE), lower epidermal cell (LE), stomata (S).

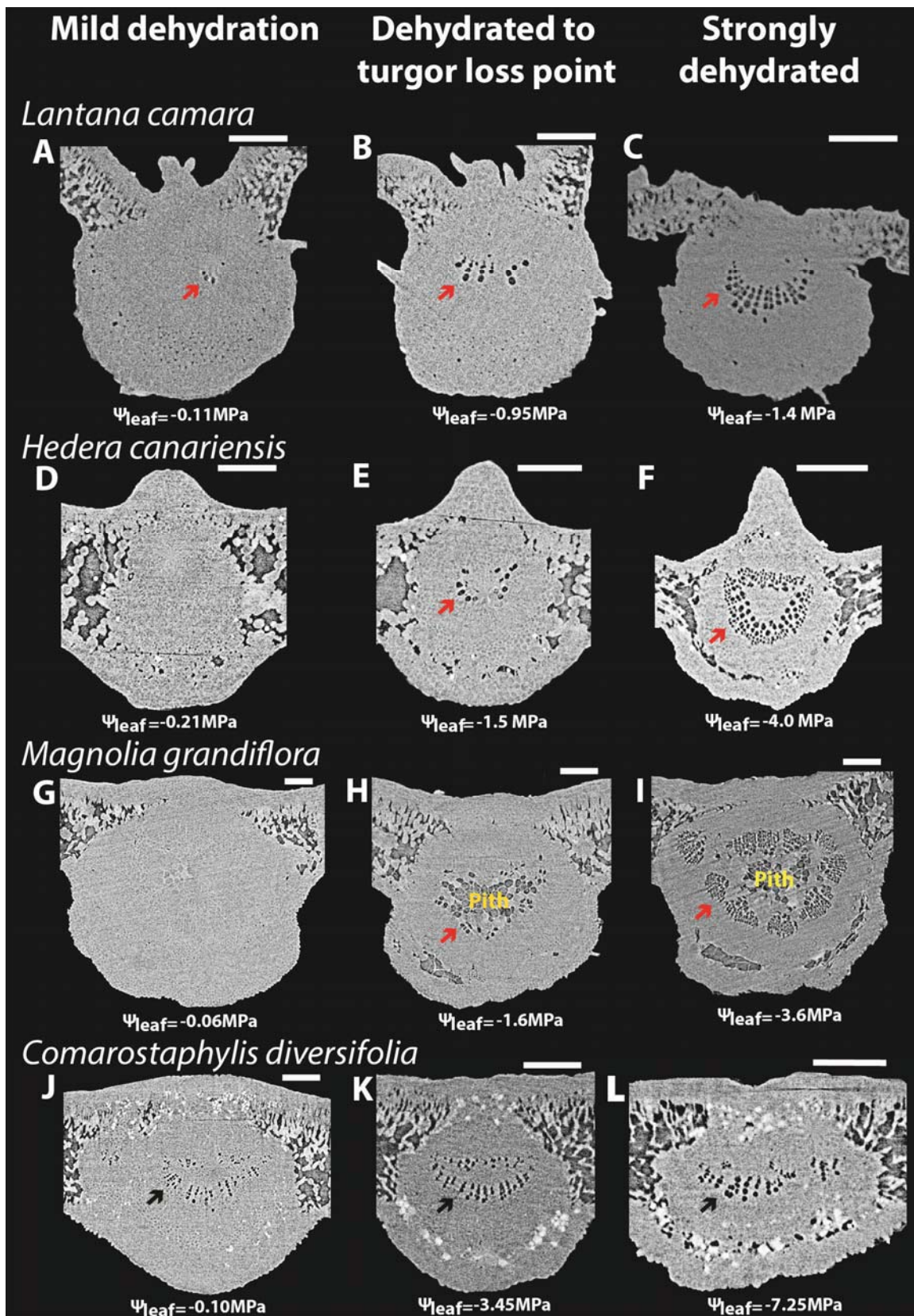


Figure 2

Figure 2. Low vulnerability of the leaf xylem to embolism before turgor loss point as revealed by *in vivo* imaging of leaves of four diverse angiosperm species subjected to progressive dehydration (i.e., increasingly negative leaf water potential, Ψ_{leaf}) using X-ray micro-computed tomography (microCT). (A-L) scans of leaf midribs at mild dehydration, turgor loss point and extreme dehydration (an illustrative image for each range is shown from left to right), showing very few embolized midrib conduits above turgor loss point. No emboli were observed in higher order veins above turgor loss point, and few were observed even in extremely dehydrated leaves (data not shown). Note that *Comarostaphylis diversifolia* contains embolized protoxylem conduits, which are hydraulically non-functional, even for well hydrated leaves, and these protoxylem conduits are included in the calculations of embolized conduits. Scale = 250 μm .

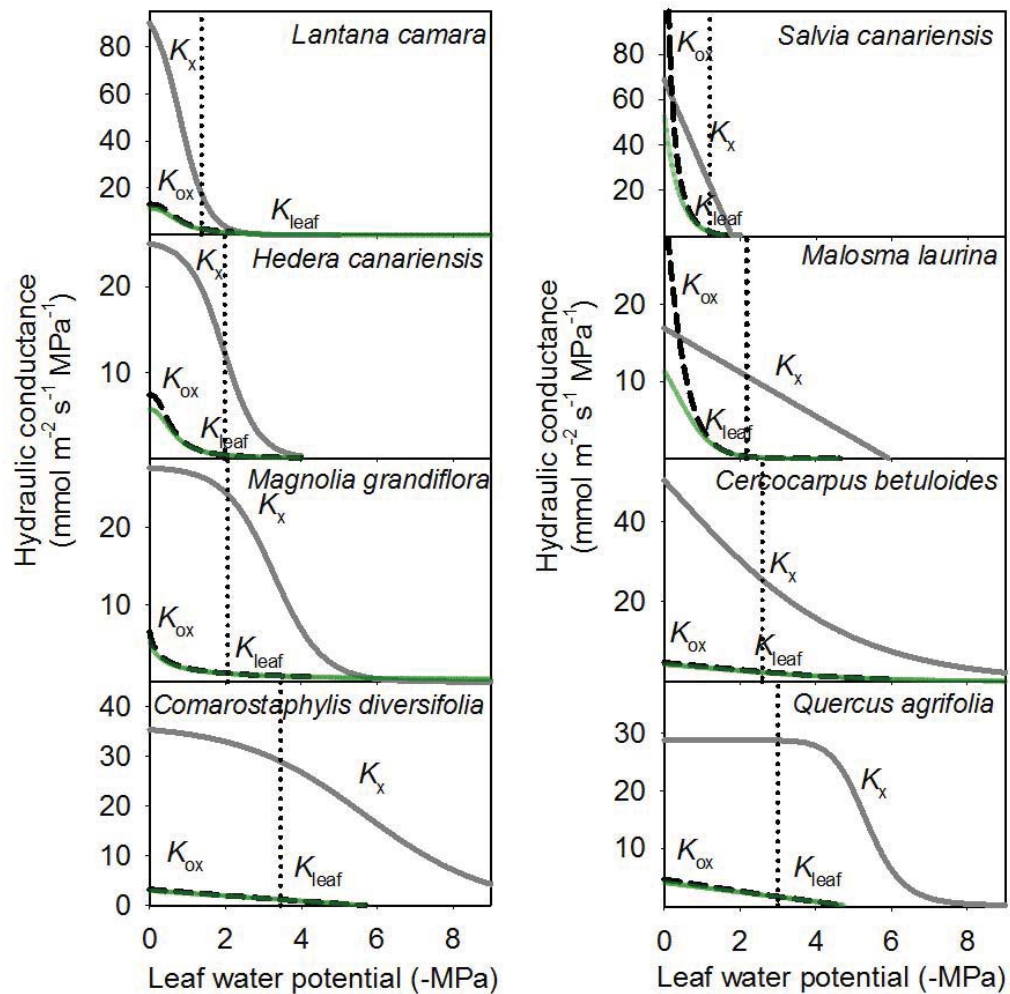


Figure 3

Figure 3. The vulnerability of whole leaf hydraulic conductance (K_{leaf} ; green) to dehydration is mainly determined by the vulnerability of the outside-xylem pathways (K_{ox} ; dashed-black), and not that of the xylem (K_x ; light grey) across the four species for which microCT was performed (left panels) and an additional expanded set of four diverse species (right panels). The maximum likelihood function is plotted for each vulnerability curve (see *Methods*). The turgor loss point for each species is represented by a dotted black line.

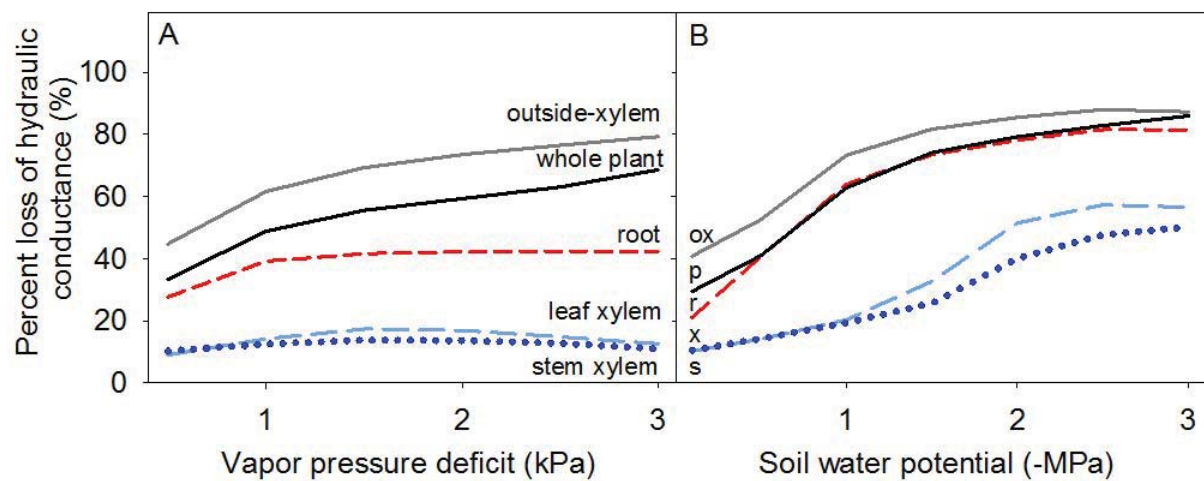


Figure 4

Figure 4. Model simulations of whole plant hydraulic response to (A) atmospheric drought (increasing vapor pressure deficit, VPD), and (B) dehydrating soil. PLC values plotted in both panels are averages of simulations obtained for the four species tested (see *Methods*). The percent loss of hydraulic conductance (PLC) outside the xylem (ox; grey solid line) is the main determinant of the decline of whole plant hydraulic conductance (p; black solid line) under both scenarios. Neither leaf xylem hydraulic conductance (x; medium dash light blue line) nor stem xylem hydraulic conductance (s; dotted dark blue line) experience strong declines with increasing soil drought or VPD. The root hydraulic conductance (small dashed red line) declines strongly under increasing soil drought, and to a smaller extent under increasing VPD. Because the model simulates a transpiring plant, when the soil water potential is at zero on the *x*-axis, the transpiring leaf water potential is still substantially negative, driving the decline of K_{leaf} from its maximum value (though not of K_x ; please see Table S2 for water potentials of each compartment). Under the soil drought scenario, VPD was maintained at 0.5 kPa. Under the atmospheric drought scenario, soil water potential was maintained at -0.1 MPa.

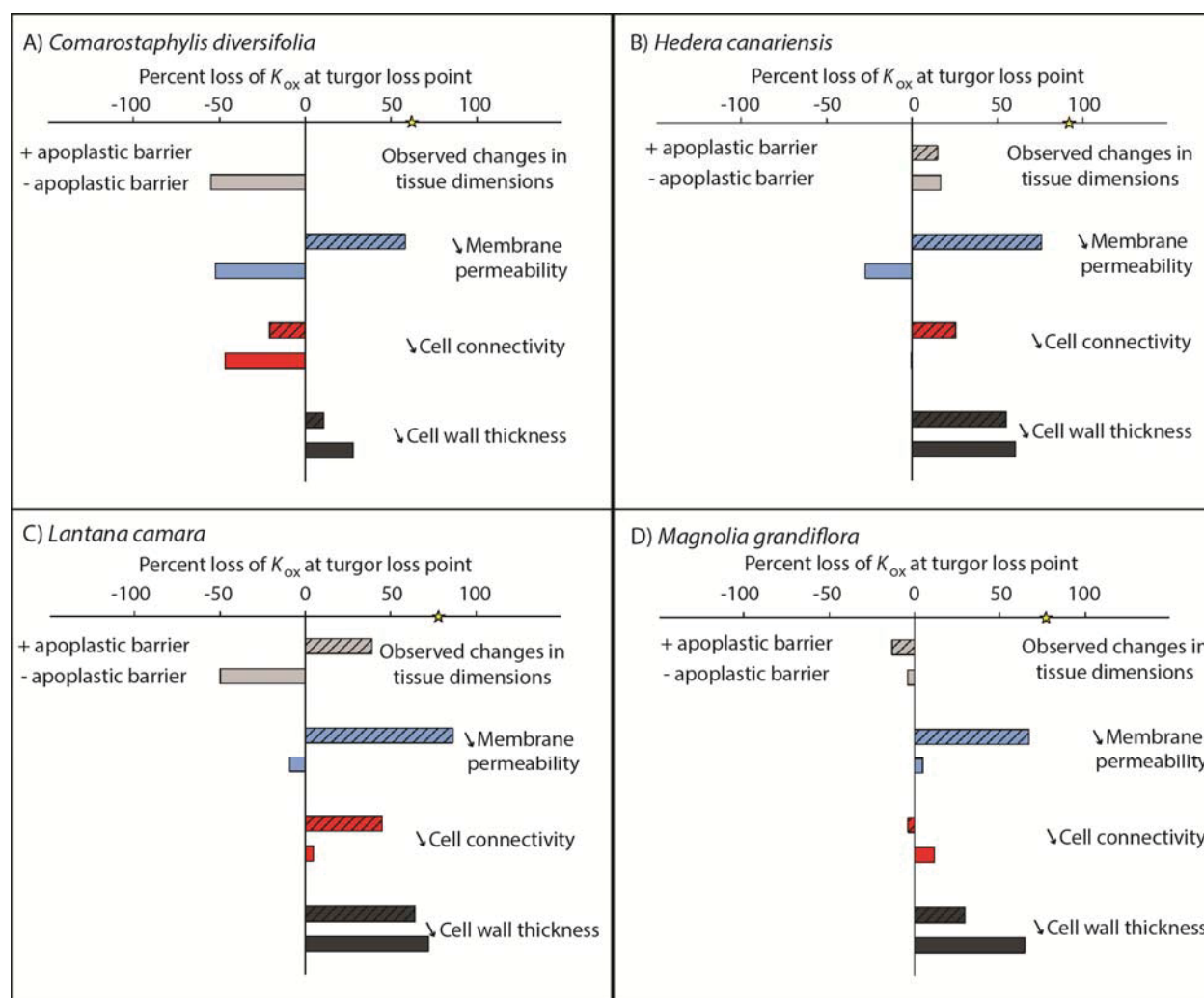


Figure 6

Figure 6. Testing hypotheses for the potential drivers of the decline in outside-xylem hydraulic conductance in dehydrating leaves, using a spatially explicit model of leaf outside-xylem water transport (*see Methods*). Parameterizing the model for four species, we estimated the outside-xylem hydraulic conductance (K_{ox}) based on the decline of observed cell size, porosity (airspace) and leaf area at turgor loss point (light grey bars). Because in some cases these changes in tissue dimensions resulted in an *increase* in K_{ox} , we modelled K_{ox} decline according to three scenarios (always including the observed changes in tissue dimension): an 80% decline at turgor loss point in membrane permeability (blue bars), cell connectivity (red bars), and cell wall thickness (dark grey bar). All simulations were run with or without including an apoplastic barrier at the bundle

sheath cells (filled vs. striped bars). The yellow star on the x -axis represents the observed % K_{ox} decline at turgor loss point. Across all four species, only simulations of a strong decrease in membrane permeability in leaves with an apoplastic barrier could explain the observed declines in K_{ox} .

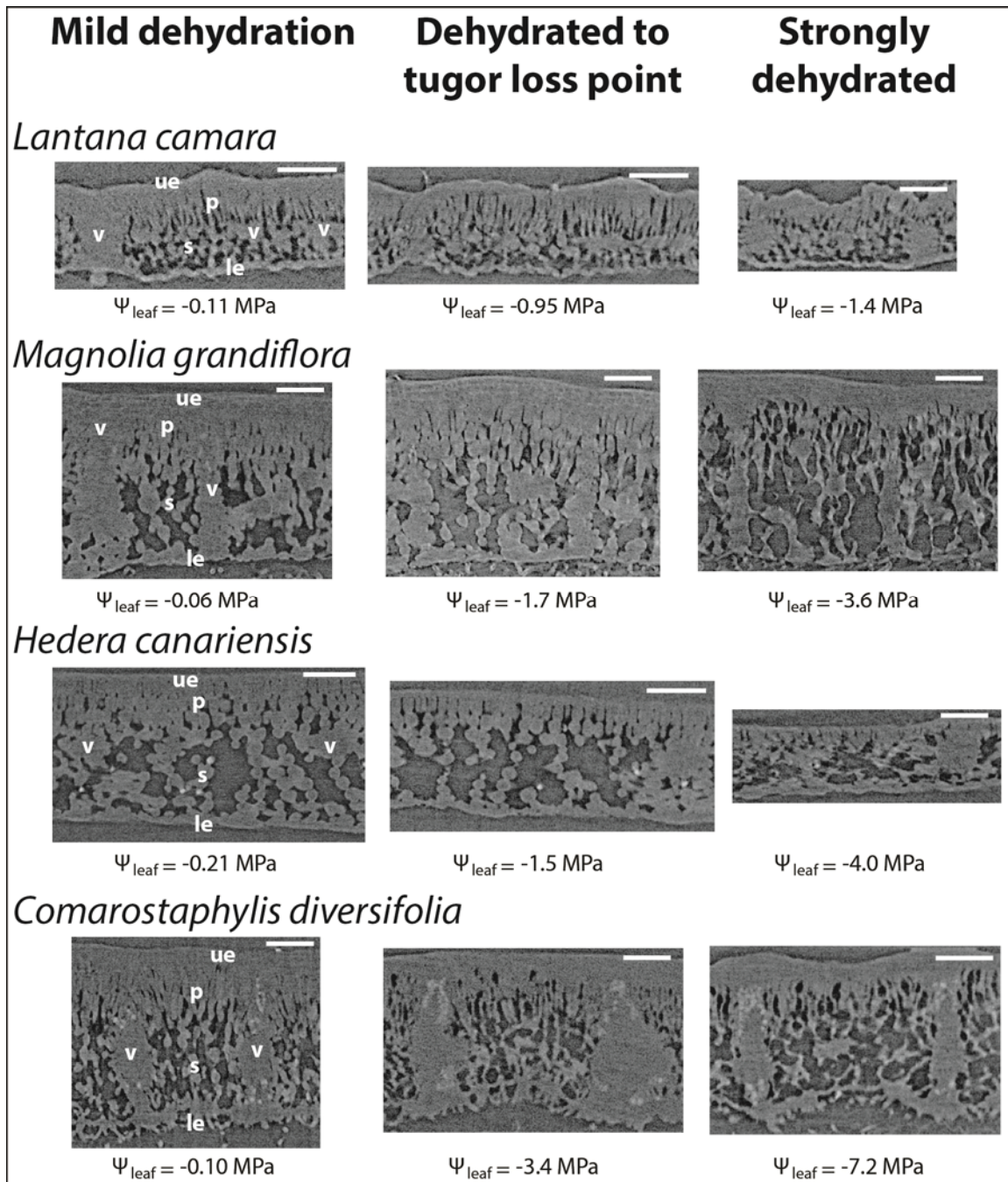


Figure 5

Figure 5. X-ray micro-computed tomography scans of leaf laminas at three dehydration levels for four species. Symbols: Leaf water potential (Ψ_{leaf}), vascular bundle (V), spongy mesophyll cell (S), palisade mesophyll cell (P), upper epidermal cell (UE), lower epidermal cell (LE). Scale = 250 μm .

Parsed Citations

Anderegg WRL, Flint A, Huang C-y, Flint L, Berry JA, Davis FW, Sperry JS, Field CB (2015) Tree mortality predicted from drought-induced vascular damage. *Nature Geoscience* 8: 367-371

Pubmed: [Author and Title](#)

CrossRef: [Author and Title](#)

Google Scholar: [Author Only](#) [Title Only](#) [Author and Title](#)

Bartlett MK, Klein T, Jansen S, Choat B, L. S (2016) The correlations and sequence of plant stomatal, hydraulic, and wilting responses to drought. *Proceedings of the National Academy of Sciences of the United States of America* 113: 13098-13103

Pubmed: [Author and Title](#)

CrossRef: [Author and Title](#)

Google Scholar: [Author Only](#) [Title Only](#) [Author and Title](#)

Bartlett MK, Scoffoni C, Sack L (2012) The determinants of leaf turgor loss point and prediction of drought tolerance of species and biomes: a global meta-analysis. *Ecology Letters* 15: 393-405

Pubmed: [Author and Title](#)

CrossRef: [Author and Title](#)

Google Scholar: [Author Only](#) [Title Only](#) [Author and Title](#)

Blackman CJ, Brodribb TJ, Jordan GJ (2010) Leaf hydraulic vulnerability is related to conduit dimensions and drought resistance across a diverse range of woody angiosperms. *New Phytologist* 188: 1113-1123

Pubmed: [Author and Title](#)

CrossRef: [Author and Title](#)

Google Scholar: [Author Only](#) [Title Only](#) [Author and Title](#)

Blackman CJ, Gleason SM, Chang Y, Cook AM, Laws C, Westoby M (2014) Leaf hydraulic vulnerability to drought is linked to site water availability across a broad range of species and climates. *Annals of Botany* 114: 435-440

Pubmed: [Author and Title](#)

CrossRef: [Author and Title](#)

Google Scholar: [Author Only](#) [Title Only](#) [Author and Title](#)

Bouche PS, Delzon S, Choat B, Bader E, Brodribb T, Burlett R, Cochard H, Charra-Vaskou K, Lavigne B, Shan L, Mayr S, Morris H, Torres-Ruiz JM, Zufferey V, Jansen S (2016) Are needles of *Pinus pinaster* more vulnerable to xylem embolism than branches? New insights from X-ray computed tomography. *Plant, Cell & Environment* 39: 860-870

Pubmed: [Author and Title](#)

CrossRef: [Author and Title](#)

Google Scholar: [Author Only](#) [Title Only](#) [Author and Title](#)

Boyer JS (1985) Water transport. In WR Briggs, ed, *Annual review of plant physiology*, Vol 36, Annual reviews Inc: Palo Alto, CA, USA, pp 473-516

Pubmed: [Author and Title](#)

CrossRef: [Author and Title](#)

Google Scholar: [Author Only](#) [Title Only](#) [Author and Title](#)

Brodribb T, Skelton RP, McAdam SAM, Bienaimé D, Lucani CJ, Marmottant P (2016a) Visual quantification of embolism reveals leaf vulnerability to hydraulic failure. *New Phytologist* doi: 10.1111/nph.13846

Pubmed: [Author and Title](#)

CrossRef: [Author and Title](#)

Google Scholar: [Author Only](#) [Title Only](#) [Author and Title](#)

Brodribb TJ, Bienaimé D, Marmottant P (2016b) Revealing catastrophic failure of leaf networks under stress. *Proceedings of the National Academy of Sciences of the United States of America* 113: 4865-4869

Pubmed: [Author and Title](#)

CrossRef: [Author and Title](#)

Google Scholar: [Author Only](#) [Title Only](#) [Author and Title](#)

Brodribb TJ, Hill RS (2000) Increases in water potential gradient reduce xylem conductivity in whole plants. Evidence from a low-pressure conductivity method. *Plant Physiology* 123: 1021-1027

Pubmed: [Author and Title](#)

CrossRef: [Author and Title](#)

Google Scholar: [Author Only](#) [Title Only](#) [Author and Title](#)

Brodribb TJ, Holbrook NM (2003) Stomatal closure during leaf dehydration, correlation with other leaf physiological traits. *Plant Physiology* 132: 2166-2173

Pubmed: [Author and Title](#)

CrossRef: [Author and Title](#)

Google Scholar: [Author Only](#) [Title Only](#) [Author and Title](#)

Brodribb TJ, Holbrook NM (2005) Water stress deforms tracheids peripheral to the leaf vein of a tropical conifer. *Plant Physiology* 137: 1139-1146

Pubmed: [Author and Title](#)

CrossRef: [Author and Title](#)

Google Scholar: [Author Only](#) [Title Only](#) [Author and Title](#)

Brodribb TJ, Holbrook NM (2006) Declining hydraulic efficiency as transpiring leaves desiccate: two types of response. *Plant Cell and Environment* 29: 2205-2215

Pubmed: [Author and Title](#)

CrossRef: [Author and Title](#)

Google Scholar: [Author Only](#) [Title Only](#) [Author and Title](#)

Brodribb TJ, McAdam SAM (2013) Absciscic Acid Mediates a Divergence in the Drought Response of Two Conifers. Plant Physiology 162: 1370-1377

Pubmed: [Author and Title](#)

CrossRef: [Author and Title](#)

Google Scholar: [Author Only](#) [Title Only](#) [Author and Title](#)

Bucci SJ, Scholz FG, Goldstein G, Meinzer FC, Sternberg LDL (2003) Dynamic changes in hydraulic conductivity in petioles of two savanna tree species: factors and mechanisms contributing to the refilling of embolized vessels. Plant Cell and Environment 26: 1633-1645

Pubmed: [Author and Title](#)

CrossRef: [Author and Title](#)

Google Scholar: [Author Only](#) [Title Only](#) [Author and Title](#)

Buckley TN (2015) The contributions of apoplastic, symplastic and gas phase pathways for water transport outside the bundle sheath in leaves. Plant Cell and Environment 38: 7-22

Pubmed: [Author and Title](#)

CrossRef: [Author and Title](#)

Google Scholar: [Author Only](#) [Title Only](#) [Author and Title](#)

Buckley TN, John GP, Scoffoni C, Sack L (2015) How Does Leaf Anatomy Influence Water Transport outside the Xylem? Plant Physiology 168: 1616-1635

Pubmed: [Author and Title](#)

CrossRef: [Author and Title](#)

Google Scholar: [Author Only](#) [Title Only](#) [Author and Title](#)

Burnham KP, Anderson DR (2004) Multimodel inference - understanding AIC and BIC in model selection. Sociological Methods & Research 33: 261-304

Pubmed: [Author and Title](#)

CrossRef: [Author and Title](#)

Google Scholar: [Author Only](#) [Title Only](#) [Author and Title](#)

Canny MJ (1986) Water pathways in Wheat leaves. 3. The passage of the mestome sheath and the function of the suberized lamellae. Physiologia Plantarum 66: 637-647

Pubmed: [Author and Title](#)

CrossRef: [Author and Title](#)

Google Scholar: [Author Only](#) [Title Only](#) [Author and Title](#)

Canny MJ (1988) Water pathways in Wheat leaves. 4. The interpretation of images of a fluorescent apoplastic tracer. Australian Journal of Plant Physiology 15: 541-555

Pubmed: [Author and Title](#)

CrossRef: [Author and Title](#)

Google Scholar: [Author Only](#) [Title Only](#) [Author and Title](#)

Charra-Vaskou K, Badel E, Burlett R, Cochard H, Delzon S, Mayr S (2012) Hydraulic efficiency and safety of vascular and non-vascular components in Pinus pinaster leaves. Tree Physiology 32: 1161-1170

Pubmed: [Author and Title](#)

CrossRef: [Author and Title](#)

Google Scholar: [Author Only](#) [Title Only](#) [Author and Title](#)

Chaumont F, Tyerman SD (2014) Aquaporins: Highly Regulated Channels Controlling Plant Water Relations. Plant Physiology 164: 1600-1618

Pubmed: [Author and Title](#)

CrossRef: [Author and Title](#)

Google Scholar: [Author Only](#) [Title Only](#) [Author and Title](#)

Choat B, Jansen S, Brodribb TJ, Cochard H, Delzon S, Bhaskar R, Bucci SJ, Feild TS, Gleason SM, Hacke UG, Jacobsen AL, Lens F, Maherali H, Martinez-Vilalta J, Mayr S, Mencuccini M, Mitchell PJ, Nardini A, Pittermann J, Pratt RB, Sperry JS, Westoby M, Wright IJ, Zanne AE (2012) Global convergence in the vulnerability of forests to drought. Nature 491: 752+

Pubmed: [Author and Title](#)

CrossRef: [Author and Title](#)

Google Scholar: [Author Only](#) [Title Only](#) [Author and Title](#)

Choat B, Lahr EC, Melcher P, Zwieniecki MA, Holbrook NM (2005) The spatial pattern of air seeding thresholds in mature sugar maple trees. Plant, Cell & Environment 28: 1082-1089

Pubmed: [Author and Title](#)

CrossRef: [Author and Title](#)

Google Scholar: [Author Only](#) [Title Only](#) [Author and Title](#)

Cochard H, Badel E, Herbette S, Delzon S, Choat B, Jansen S (2013) Methods for measuring plant vulnerability to cavitation: a critical review. Journal of Experimental Botany 64: 4779-4791

Pubmed: [Author and Title](#)

CrossRef: [Author and Title](#)

Google Scholar: [Author Only](#) [Title Only](#) [Author and Title](#)

Cochard H, Bodet C, Ameglio T, Cruiziat P (2000) Cryo-scanning electron microscopy observations of vessel content during transpiration in walnut petioles. Facts or artifacts? Plant Physiology 124: 1191-1202

Pubmed: [Author and Title](#)

CrossRef: [Author and Title](#)

Google Scholar: [Author Only](#) [Title Only](#) [Author and Title](#)

Cochard H, Venisse JS, Barigah TS, Brunel N, Herbette S, Guilliot A, Tyree MT, Sakr S (2007) Putative role of aquaporins in variable hydraulic conductance of leaves in response to light. Plant Physiology 143: 122-133

Pubmed: [Author and Title](#)

CrossRef: [Author and Title](#)

Google Scholar: [Author Only](#) [Title Only](#) [Author and Title](#)

Coomes DA, S. H, E.R. G, J.J. S, Sack L (2008) Scaling of xylem vessels and veins within the leaves of oak species. Biology Letters 4: 302-306

Pubmed: [Author and Title](#)

CrossRef: [Author and Title](#)

Google Scholar: [Author Only](#) [Title Only](#) [Author and Title](#)

Crombie DS, Milburn JA, Hipkins MF (1985) Maximum sustainable xylem sap tensions in Rhododendron and other species. Planta 163: 27-33

Pubmed: [Author and Title](#)

CrossRef: [Author and Title](#)

Google Scholar: [Author Only](#) [Title Only](#) [Author and Title](#)

Cuneo IF, Knipfer T, Brodersen C, McElrone AJ (2016) Mechanical failure of fine root cortical cells initiates plant hydraulic decline during drought. Plant Physiology doi:10.1104/pp.16.00923

Pubmed: [Author and Title](#)

CrossRef: [Author and Title](#)

Google Scholar: [Author Only](#) [Title Only](#) [Author and Title](#)

Diffenbaugh NS, Swain DL, Torma D (2015) Anthropogenic warming has increased drought risk in California. Proceedings of the National Academy of Sciences of the United States of America 112: 3931-3936

Pubmed: [Author and Title](#)

CrossRef: [Author and Title](#)

Google Scholar: [Author Only](#) [Title Only](#) [Author and Title](#)

Dixon HH, Joly J (1895) On the ascent of sap. Philosophical Transactions of the Royal Society of London 186: 563-576

Pubmed: [Author and Title](#)

CrossRef: [Author and Title](#)

Google Scholar: [Author Only](#) [Title Only](#) [Author and Title](#)

Guyot G, Scoffoni C, Sack L (2012) Combined impacts of irradiance and dehydration on leaf hydraulic conductance: insights into vulnerability and stomatal control. Plant, Cell & Environment 35: 857-871

Pubmed: [Author and Title](#)

CrossRef: [Author and Title](#)

Google Scholar: [Author Only](#) [Title Only](#) [Author and Title](#)

Hacke UG, Sperry JS, Pittermann J (2000) Drought experience and cavitation resistance in six shrubs from the Great Basin, Utah. Basic and Applied Ecology 1: 31-41

Pubmed: [Author and Title](#)

CrossRef: [Author and Title](#)

Google Scholar: [Author Only](#) [Title Only](#) [Author and Title](#)

Hernandez-Santana V, Rodriguez-Dominguez CM, Fernández JE, Diaz-Espejo A (2016) Role of leaf hydraulic conductance in the regulation of stomatal conductance in almond and olive in response to water stress. Tree Physiology 00: 1-11

Pubmed: [Author and Title](#)

CrossRef: [Author and Title](#)

Google Scholar: [Author Only](#) [Title Only](#) [Author and Title](#)

Hochberg U, Albuquerque C, Rachmilevitch S, Cochard H, David-Schwartz R, Brodersen CR, McElrone A, Windt CW (2016) Grapevine petioles are more sensitive to drought induced embolism than stems: evidence from in vivo MRI and microcomputed tomography observations of hydraulic vulnerability segmentation. Plant, Cell & Environment: n/a-n/a

Pubmed: [Author and Title](#)

CrossRef: [Author and Title](#)

Google Scholar: [Author Only](#) [Title Only](#) [Author and Title](#)

Johansson I, Karlsson M, Shukla VK, Chrispeels MJ, Larsson C, Kjellbom P (1998) Water transport activity of the plasma membrane aquaporin PM28A is regulated by phosphorylation. Plant Cell 10: 451-459

Pubmed: [Author and Title](#)

CrossRef: [Author and Title](#)

Google Scholar: [Author Only](#) [Title Only](#) [Author and Title](#)

John GP, Scoffoni C, Sack L (2013) Allometry of cells and tissues within leaves. American Journal of Botany: 100: 1936-1948

Pubmed: [Author and Title](#)

CrossRef: [Author and Title](#)

Google Scholar: [Author Only](#) [Title Only](#) [Author and Title](#)

Johnson DM, McCulloh KA, Woodruff DR, Meinzer FC (2012) Evidence for xylem embolism as a primary factor in dehydration-induced declines in leaf hydraulic conductance. Plant Cell and Environment 35: 760-769

Pubmed: [Author and Title](#)

CrossRef: [Author and Title](#)

Google Scholar: [Author Only](#) [Title Only](#) [Author and Title](#)

Johnson DM, Meinzer FC, Woodruff DR, McCulloh KA (2009a) Leaf xylem embolism, detected acoustically and by cryo-SEM, corresponds to decreases in leaf hydraulic conductance in four evergreen species. Plant, Cell and Environment 32: 828-836

Pubmed: [Author and Title](#)
CrossRef: [Author and Title](#)
Google Scholar: [Author Only](#) [Title Only](#) [Author and Title](#)

Johnson DM, Woodruff DR, McCulloh KA, Meinzer FC (2009b) Leaf hydraulic conductance, measured in situ, declines and recovers daily: leaf hydraulics, water potential and stomatal conductance in four temperate and three tropical tree species. Tree Physiology 29: 879-887

Pubmed: [Author and Title](#)
CrossRef: [Author and Title](#)
Google Scholar: [Author Only](#) [Title Only](#) [Author and Title](#)

Kikuta SB, LoGullo MA, Nardini A, Richter H, Salleo S (1997) Ultrasound acoustic emissions from dehydrating leaves of deciduous and evergreen trees. Plant Cell and Environment 20: 1381-1390

Pubmed: [Author and Title](#)
CrossRef: [Author and Title](#)
Google Scholar: [Author Only](#) [Title Only](#) [Author and Title](#)

Kim YX, Steudle E (2007) Light and turgor affect the water permeability (aquaporins) of parenchyma cells in the midrib of leaves of Zea mays. Journal of Experimental Botany 58: 4119-4129

Pubmed: [Author and Title](#)
CrossRef: [Author and Title](#)
Google Scholar: [Author Only](#) [Title Only](#) [Author and Title](#)

Kim YX, Steudle E (2009) Gating of aquaporins by light and reactive oxygen species in leaf parenchyma cells of the midrib of Zea mays. Journal of Experimental Botany 60: 547-556

Pubmed: [Author and Title](#)
CrossRef: [Author and Title](#)
Google Scholar: [Author Only](#) [Title Only](#) [Author and Title](#)

Knipfer T, Cuneo IF, Brodersen CR, McElrone AJ (2016) In situ visualization of the dynamics in xylem embolism formation and removal in the absence of root pressure: a study on excised grapevine stems. Plant Physiology 171: 1024-1036

Pubmed: [Author and Title](#)
CrossRef: [Author and Title](#)
Google Scholar: [Author Only](#) [Title Only](#) [Author and Title](#)

Laur J, Hacke UG (2014) Exploring Picea glauca aquaporins in the context of needle water uptake and xylem refilling. New Phytologist 203: 388-400

Pubmed: [Author and Title](#)
CrossRef: [Author and Title](#)
Google Scholar: [Author Only](#) [Title Only](#) [Author and Title](#)

Lersten NR (1997) Occurrence of endodermis with a casparian strip in stem and leaf. Botanical Review 63: 265-272

Pubmed: [Author and Title](#)
CrossRef: [Author and Title](#)
Google Scholar: [Author Only](#) [Title Only](#) [Author and Title](#)

Lo Gullo MA, Nardini A, Trifilo P, Salleo S (2003) Changes in leaf hydraulics and stomatal conductance following drought stress and irrigation in Ceratonia siliqua (Carob tree). Physiologia Plantarum 117: 186-194

Pubmed: [Author and Title](#)
CrossRef: [Author and Title](#)
Google Scholar: [Author Only](#) [Title Only](#) [Author and Title](#)

Maurel C, Boursiac Y, Luu D-T, Santoni V, Shahzad Z, Verdoucq L (2015) Aquaporins in Plants. Physiological reviews 95: 1321-1358

Pubmed: [Author and Title](#)
CrossRef: [Author and Title](#)
Google Scholar: [Author Only](#) [Title Only](#) [Author and Title](#)

McAdam SAM, Brodribb TJ (2014) Separating Active and Passive Influences on Stomatal Control of Transpiration. Plant Physiology 164: 1578-1586

Pubmed: [Author and Title](#)
CrossRef: [Author and Title](#)
Google Scholar: [Author Only](#) [Title Only](#) [Author and Title](#)

McKown Athena D, Cochard H, Sack L (2010) Decoding leaf hydraulics with a spatially explicit model: principles of venation architecture and implications for its evolution. The American Naturalist 175: 447-460

Pubmed: [Author and Title](#)
CrossRef: [Author and Title](#)
Google Scholar: [Author Only](#) [Title Only](#) [Author and Title](#)

Milburn JA (1966) Conduction of sap. I. Water conduction and cavitation in water stressed leaves. Planta 69: 34-&

Pubmed: [Author and Title](#)
CrossRef: [Author and Title](#)
Google Scholar: [Author Only](#) [Title Only](#) [Author and Title](#)

Milburn JA, Johnson RPC (1966) Conductance of sap. 2. Detection of vibrations produced by sap cavitation in Ricinus xylem. Planta 69: 43-52

Pubmed: [Author and Title](#)
CrossRef: [Author and Title](#)
Google Scholar: [Author Only](#) [Title Only](#) [Author and Title](#)

Miyazawa S, Yoshimura S, Shimazaki Y, Maeshima M, Miyake C (2008) Deactivation of aquaporins decreases internal conductance to
Copyright © 2017 American Society of Plant Biologists. All rights reserved.

CO2 diffusion in tobacco leaves grown under long-term drought. Functional Plant Biology 35: 553-564

Pubmed: [Author and Title](#)
CrossRef: [Author and Title](#)
Google Scholar: [Author Only Title Only Author and Title](#)

Moshelion M, Halperin O, Wallach R, Oren R, Way DA (2015) Role of aquaporins in determining transpiration and photosynthesis in water-stressed plants: crop water-use efficiency, growth and yield. Plant Cell and Environment 38: 1785-1793

Pubmed: [Author and Title](#)
CrossRef: [Author and Title](#)
Google Scholar: [Author Only Title Only Author and Title](#)

Murray K, Conner MM (2009) Methods to quantify variable importance: implications for the analysis of noisy ecological data Ecology 90: 348-355

Pubmed: [Author and Title](#)
CrossRef: [Author and Title](#)
Google Scholar: [Author Only Title Only Author and Title](#)

Nardini A, Ramani M, Gortan E, Salleo S (2008) Vein recovery from embolism occurs under negative pressure in leaves of sunflower (*Helianthus annuus*). Physiologia Plantarum 133: 755-764

Pubmed: [Author and Title](#)
CrossRef: [Author and Title](#)
Google Scholar: [Author Only Title Only Author and Title](#)

Nardini A, Salleo S (2000) Limitation of stomatal conductance by hydraulic traits: sensing or preventing xylem cavitation? Trees-Structure and Function 15: 14-24

Pubmed: [Author and Title](#)
CrossRef: [Author and Title](#)
Google Scholar: [Author Only Title Only Author and Title](#)

Nardini A, Salleo S (2003) Effects of the experimental blockage of the major veins on hydraulics and gas exchange of *Prunus laurocerasus* L. leaves. Journal of Experimental Botany 54: 1213-1219

Pubmed: [Author and Title](#)
CrossRef: [Author and Title](#)
Google Scholar: [Author Only Title Only Author and Title](#)

Nardini A, Salleo S, Raimondo F (2003) Changes in leaf hydraulic conductance correlate with leaf vein embolism in *Cercis siliquastrum* L. Trees-Structure and Function 17: 529-534

Pubmed: [Author and Title](#)
CrossRef: [Author and Title](#)
Google Scholar: [Author Only Title Only Author and Title](#)

Nardini A, Tyree MT, Salleo S (2001) Xylem cavitation in the leaf of *Prunus laurocerasus* and its impact on leaf hydraulics. Plant Physiology 125: 1700-1709

Pubmed: [Author and Title](#)
CrossRef: [Author and Title](#)
Google Scholar: [Author Only Title Only Author and Title](#)

North GB, Martre P, Nobel PS (2004) Aquaporins account for variations in hydraulic conductance for metabolically active root regions of *Agave deserti* in wet, dry, and rewetted soil. Plant Cell and Environment 27: 219-228

Pubmed: [Author and Title](#)
CrossRef: [Author and Title](#)
Google Scholar: [Author Only Title Only Author and Title](#)

Osborne CP, Sack L (2012) Evolution of C-4 plants: a new hypothesis for an interaction of CO2 and water relations mediated by plant hydraulics. Philosophical Transactions of the Royal Society B-Biological Sciences 367: 583-600

Pubmed: [Author and Title](#)
CrossRef: [Author and Title](#)
Google Scholar: [Author Only Title Only Author and Title](#)

Pammenter NW, Vander Willigen C (1998) A mathematical and statistical analysis of the curves illustrating vulnerability of xylem to cavitation. Tree Physiology 18: 589-593

Pubmed: [Author and Title](#)
CrossRef: [Author and Title](#)
Google Scholar: [Author Only Title Only Author and Title](#)

Pantin F, Monnet F, Jannaud D, Costa JM, Renaud J, Muller B, Simonneau T, Genty B (2013) The dual effect of abscisic acid on stomata. New Phytologist 197: 65-72

Pubmed: [Author and Title](#)
CrossRef: [Author and Title](#)
Google Scholar: [Author Only Title Only Author and Title](#)

Pierce M, Raschke K (1980) Correlation between loss of turgor and accumulation of abscisic acid in detached leaves. Planta 148: 174-182

Pubmed: [Author and Title](#)
CrossRef: [Author and Title](#)
Google Scholar: [Author Only Title Only Author and Title](#)

Pieruschka R, Huber G, Berry JA (2010) Control of transpiration by radiation. Proceedings of the National Academy of Sciences of the United States of America 107: 13372-13377

Pubmed: [Author and Title](#)

CrossRef: [Author and Title](#)
Google Scholar: [Author Only](#) [Title Only](#) [Author and Title](#)

Pou A, Medrano H, Flexas J, Tyerman SD (2013) A putative role for TIP and PIP aquaporins in dynamics of leaf hydraulic and stomatal conductances in grapevine under water stress and re-watering. Plant Cell and Environment 36: 828-843

Pubmed: [Author and Title](#)
CrossRef: [Author and Title](#)
Google Scholar: [Author Only](#) [Title Only](#) [Author and Title](#)

Prado K, Maurel C (2013) Regulation of leaf hydraulics: from molecular to whole plant levels. Frontiers in plant science 4

Pubmed: [Author and Title](#)
CrossRef: [Author and Title](#)
Google Scholar: [Author Only](#) [Title Only](#) [Author and Title](#)

Ribeiro MLRC, Santos MG, Moraes MG (2007) Leaf anatomy of two Anemia Sw. species (Schizaeaceae-Pteridophyte) from a rocky outcrop in Niteroi, Rio de Janeiro, Brazil. Revista Brasileira de Botanica 30: 695-702

Pubmed: [Author and Title](#)
CrossRef: [Author and Title](#)
Google Scholar: [Author Only](#) [Title Only](#) [Author and Title](#)

Ritman KT, Milburn JA (1988) Acoustic emissions from plants- Ultrasonic and audible compared. Journal of Experimental Botany 39: 1237-1248

Pubmed: [Author and Title](#)
CrossRef: [Author and Title](#)
Google Scholar: [Author Only](#) [Title Only](#) [Author and Title](#)

Rockwell FE, Holbrook NM, Stroock AD (2014) The Competition between Liquid and Vapor Transport in Transpiring Leaves. Plant Physiology 164: 1741-1758

Pubmed: [Author and Title](#)
CrossRef: [Author and Title](#)
Google Scholar: [Author Only](#) [Title Only](#) [Author and Title](#)

Sack L, Ball MC, Brodersen C, Donovan L, Givnish TJ, Hacke U, Huxman TE, Jacobsen AL, Jansen S, Johnson DM, G. K, Lachenbruch B, Maurel C, McCulloch KA, McDowell N, McElrone AJ, Meinzer F, Melcher P, North GB, Pellegrini M, Pockman WT, Pratt RB, Rockwell FE, Sala A, Santiago LS, Scoffoni C, Sevanto SA, Sperry J, Spicer RA, Davies SJ, Tyerman SD, Way DA, Zweiniecki MA, Holbrook MN (2016a) Plant water transport as a central hub from plant to ecosystem function: meeting report for "Emerging Frontiers in Plant Hydraulics" (Washington, DC, May 2015). Plant, Cell & Environment: In Press.

Pubmed: [Author and Title](#)
CrossRef: [Author and Title](#)
Google Scholar: [Author Only](#) [Title Only](#) [Author and Title](#)

Sack L, Buckley TN, Scoffoni C (2016b) Why are leaves hydraulically vulnerable? Journal of Experimental Botany 67: 4917-4919

Pubmed: [Author and Title](#)
CrossRef: [Author and Title](#)
Google Scholar: [Author Only](#) [Title Only](#) [Author and Title](#)

Sack L, Holbrook NM (2006) Leaf hydraulics. Annual Review of Plant Biology 57: 361-381

Pubmed: [Author and Title](#)
CrossRef: [Author and Title](#)
Google Scholar: [Author Only](#) [Title Only](#) [Author and Title](#)

Sack L, Melcher PJ, Zwieniecki MA, Holbrook NM (2002) The hydraulic conductance of the angiosperm leaf lamina: a comparison of three measurement methods. Journal of Experimental Botany 53: 2177-2184

Pubmed: [Author and Title](#)
CrossRef: [Author and Title](#)
Google Scholar: [Author Only](#) [Title Only](#) [Author and Title](#)

**Sack L, PrometheusWiki (2010) Leaf pressure-volume curve parameters In. PrometheusWiki
[http://www.publish.csiro.au/prometheuswiki/tiki-pagehistory.php?page=Leaf pressure-volume curve parameters&preview=10](http://www.publish.csiro.au/prometheuswiki/tiki-pagehistory.php?page=Leaf+pressure-volume+curve+parameters&preview=10)**

Pubmed: [Author and Title](#)
CrossRef: [Author and Title](#)
Google Scholar: [Author Only](#) [Title Only](#) [Author and Title](#)

Sack L, Scoffoni C (2012) Measurement of leaf hydraulic conductance and stomatal conductance and their responses to irradiance and dehydration using the evaporative flux methods (EFM). Journal of Visualized Experiments e4179: 1-7

Pubmed: [Author and Title](#)
CrossRef: [Author and Title](#)
Google Scholar: [Author Only](#) [Title Only](#) [Author and Title](#)

Sack L, Scoffoni C (2013) Leaf venation: structure, function, development, evolution, ecology and applications in past, present and future. New Phytologist 198: 938-1000

Pubmed: [Author and Title](#)
CrossRef: [Author and Title](#)
Google Scholar: [Author Only](#) [Title Only](#) [Author and Title](#)

Sack L, Streeter CM, Holbrook NM (2004) Hydraulic analysis of water flow through leaves of sugar maple and red oak. Plant Physiology 134: 1824-1833

Pubmed: [Author and Title](#)
CrossRef: [Author and Title](#)
Google Scholar: [Author Only](#) [Title Only](#) [Author and Title](#)

Sade N, Shatil-Cohen A, Attia Z, Maurel C, Boursiac Y, Kelly G, Granot D, Yaaran A, Lerner S, Moshelion M (2014) The Role of Plasma Membrane Aquaporins in Regulating the Bundle Sheath-Mesophyll Continuum and Leaf Hydraulics. Plant Physiology 166: 1609-+

Pubmed: [Author and Title](#)

CrossRef: [Author and Title](#)

Google Scholar: [Author Only](#) [Title Only](#) [Author and Title](#)

Sade N, Shatil-Cohen A, Moshelion M (2015) Bundle-sheath aquaporins play a role in controlling Arabidopsis leaf hydraulic conductivity. Plant Signaling & Behavior 10

Pubmed: [Author and Title](#)

CrossRef: [Author and Title](#)

Google Scholar: [Author Only](#) [Title Only](#) [Author and Title](#)

Salleo S, Lo Gullo MA, Raimondo F, Nardini A (2001) Vulnerability to cavitation of leaf minor veins: any impact on leaf gas exchange? Plant Cell and Environment 24: 851-859

Pubmed: [Author and Title](#)

CrossRef: [Author and Title](#)

Google Scholar: [Author Only](#) [Title Only](#) [Author and Title](#)

Salleo S, Nardini A, Pitt F, Lo Gullo MA (2000) Xylem cavitation and hydraulic control of stomatal conductance in Laurel (Laurus nobilis L.). Plant Cell and Environment 23: 71-79

Pubmed: [Author and Title](#)

CrossRef: [Author and Title](#)

Google Scholar: [Author Only](#) [Title Only](#) [Author and Title](#)

Sancho-Knapik D, Alvarez-Arenas TG, Peguero-Pina JJ, Fernandez V, Gil-Pelegrin E (2011) Relationship between ultrasonic properties and structural changes in the mesophyll during leaf dehydration. Journal of Experimental Botany 62: 3637-3645

Pubmed: [Author and Title](#)

CrossRef: [Author and Title](#)

Google Scholar: [Author Only](#) [Title Only](#) [Author and Title](#)

Sandford AP, Grace J (1985) The measurement and interpretation of ultrasound from woody stems. Journal of Experimental Botany 36: 298-311

Pubmed: [Author and Title](#)

CrossRef: [Author and Title](#)

Google Scholar: [Author Only](#) [Title Only](#) [Author and Title](#)

Scoffoni C, Albuquerque C, Brodersen CR, Townes ST, John GP, Cochard H, Buckley TN, McElrone AJ, L. S (2016) Leaf vein xylem conduit diameter influences susceptibility to embolism and hydraulic decline. New Phytologist: doi:10.1111/nph.14256

Pubmed: [Author and Title](#)

CrossRef: [Author and Title](#)

Google Scholar: [Author Only](#) [Title Only](#) [Author and Title](#)

Scoffoni C, McKown AD, Rawls M, Sack L (2012) Dynamics of leaf hydraulic conductance with water status: quantification and analysis of species differences under steady-state. Journal of Experimental Botany 63: 643-658

Pubmed: [Author and Title](#)

CrossRef: [Author and Title](#)

Google Scholar: [Author Only](#) [Title Only](#) [Author and Title](#)

Scoffoni C, Pou A, Aasamaa K, Sack L (2008) The rapid light response of leaf hydraulic conductance: new evidence from two experimental methods. Plant Cell and Environment 31: 1803-1812

Pubmed: [Author and Title](#)

CrossRef: [Author and Title](#)

Google Scholar: [Author Only](#) [Title Only](#) [Author and Title](#)

Scoffoni C, Rawls M, McKown A, Cochard H, Sack L (2011) Decline of leaf hydraulic conductance with dehydration: relationship to leaf size and venation architecture. Plant Physiology 156: 832-843

Pubmed: [Author and Title](#)

CrossRef: [Author and Title](#)

Google Scholar: [Author Only](#) [Title Only](#) [Author and Title](#)

Scoffoni C, Sack L (2015) Are leaves "freewheelin'"? Testing for a Wheeler-type effect in leaf xylem hydraulic decline. Plant, Cell & Environment 38: 534-543

Pubmed: [Author and Title](#)

CrossRef: [Author and Title](#)

Google Scholar: [Author Only](#) [Title Only](#) [Author and Title](#)

Scoffoni C, Vuong C, Diep S, Cochard H, Sack L (2014) Leaf shrinkage with dehydration: coordination with hydraulic vulnerability and drought tolerance. Plant Physiology 164: 1772-1788

Pubmed: [Author and Title](#)

CrossRef: [Author and Title](#)

Google Scholar: [Author Only](#) [Title Only](#) [Author and Title](#)

Shatil-Cohen A, Attia Z, Moshelion M (2011) Bundle-sheath cell regulation of xylem-mesophyll water transport via aquaporins under drought stress: a target of xylem-borne ABA? Plant Journal 67: 72-80

Pubmed: [Author and Title](#)

CrossRef: [Author and Title](#)

Google Scholar: [Author Only](#) [Title Only](#) [Author and Title](#)

Shatil-Cohen A, Moshelion M (2012) Smart pipes: the bundle sheath role as xylem-mesophyll barrier. Plant signaling & behavior 7:

Downloaded from www.plantphysiol.org on January 9, 2017 - Published by www.plantphysiol.org

Copyright © 2017 American Society of Plant Biologists. All rights reserved.

1088-1091

Pubmed: [Author and Title](#)
CrossRef: [Author and Title](#)
Google Scholar: [Author Only](#) [Title Only](#) [Author and Title](#)

Sheffield J, Wood EF, Roderick ML (2012) Little change in global drought over the past 60 years. *Nature* 491: 435+

Pubmed: [Author and Title](#)
CrossRef: [Author and Title](#)
Google Scholar: [Author Only](#) [Title Only](#) [Author and Title](#)

Stiller V, Lafitte HR, Sperry JS (2003) Hydraulic properties of rice and the response of gas exchange to water stress. *Plant Physiology* 132: 1698-1706

Pubmed: [Author and Title](#)
CrossRef: [Author and Title](#)
Google Scholar: [Author Only](#) [Title Only](#) [Author and Title](#)

Taneda H, Raj Kandel D, Ishida A, Ikeda H (2016) Altitudinal changes in leaf hydraulic conductance across five *Rhododendron* species in eastern Nepal. *Tree Physiology* In Press

Pubmed: [Author and Title](#)
CrossRef: [Author and Title](#)
Google Scholar: [Author Only](#) [Title Only](#) [Author and Title](#)

Taneda H, Terashima I (2012) Co-ordinated development of the leaf midrib xylem with the lamina in *Nicotiana tabacum*. *Annals of Botany* 110: 35-45

Pubmed: [Author and Title](#)
CrossRef: [Author and Title](#)
Google Scholar: [Author Only](#) [Title Only](#) [Author and Title](#)

Trifilo P, Gasco A, Raimondo F, Nardini A, Salleo S (2003a) Kinetics of recovery of leaf hydraulic conductance and vein functionality from cavitation-induced embolism in sunflower. *Journal of Experimental Botany* 54: 2323-2330

Pubmed: [Author and Title](#)
CrossRef: [Author and Title](#)
Google Scholar: [Author Only](#) [Title Only](#) [Author and Title](#)

Trifilo P, Nardini A, Lo Gullo MA, Salleo S (2003b) Vein cavitation and stomatal behaviour of sunflower (*Helianthus annuus*) leaves under water limitation. *Physiologia Plantarum* 119: 409-417

Pubmed: [Author and Title](#)
CrossRef: [Author and Title](#)
Google Scholar: [Author Only](#) [Title Only](#) [Author and Title](#)

Trifilo P, Raimondo F, Savi T, Lo Gullo MA, Nardini A (2016) The contribution of vascular and extra-vascular water pathways to drought-induced decline of leaf hydraulic conductance. *Journal of Experimental Botany* In Press

Pubmed: [Author and Title](#)
CrossRef: [Author and Title](#)
Google Scholar: [Author Only](#) [Title Only](#) [Author and Title](#)

Tyree MT, Ewers FW (1991) The hydraulic architecture of trees and other woody-plants. *New Phytologist* 119: 345-360

Pubmed: [Author and Title](#)
CrossRef: [Author and Title](#)
Google Scholar: [Author Only](#) [Title Only](#) [Author and Title](#)

Tyree MT, Sperry JS (1989) Vulnerability of xylem to cavitation and embolism. *Annual Review of Plant Physiology and Plant Molecular Biology* 40: 19-38

Pubmed: [Author and Title](#)
CrossRef: [Author and Title](#)
Google Scholar: [Author Only](#) [Title Only](#) [Author and Title](#)

Tyree MT, Yianoulis P (1980) The site of water evaporation from sub-stomatal cavities, liquid path resistances and hydroactive stomatal closure. *Annals of Botany* 46: 175-193

Pubmed: [Author and Title](#)
CrossRef: [Author and Title](#)
Google Scholar: [Author Only](#) [Title Only](#) [Author and Title](#)

Tyree MT, Zimmermann MH (2002) *Xylem Structure and the Ascent of Sap*. Springer, Berlin, Germany.

Pubmed: [Author and Title](#)
CrossRef: [Author and Title](#)
Google Scholar: [Author Only](#) [Title Only](#) [Author and Title](#)

Urli M, Porte AJ, Cochard H, Guengant Y, Burlett R, Delzon S (2013) Xylem embolism threshold for catastrophic hydraulic failure in angiosperm trees. *Tree Physiology* 33: 672-683

Pubmed: [Author and Title](#)
CrossRef: [Author and Title](#)
Google Scholar: [Author Only](#) [Title Only](#) [Author and Title](#)

Vandeleur RK, Sullivan W, Athman A, Jordans C, Gilliham M, Kaiser BN, Tyerman SD (2014) Rapid shoot-to-root signalling regulates root hydraulic conductance via aquaporins. *Plant Cell and Environment* 37: 520-538

Pubmed: [Author and Title](#)
CrossRef: [Author and Title](#)
Google Scholar: [Author Only](#) [Title Only](#) [Author and Title](#)

Vicente-Serrano SM, Lopez-Moreno JJ, Begueria S, Lorenzo-Lacort J, Sanchez-Lorenzo A, Garcia-Ruiz JM, Azorin-Molina C,

Moran-Tejeda E, Revuelto J, Trigo R, Coelho F, Espejo F (2014) Evidence of increasing drought severity caused by temperature rise in southern Europe. Environmental Research Letters 9

Pubmed: [Author and Title](#)

CrossRef: [Author and Title](#)

Google Scholar: [Author Only](#) [Title Only](#) [Author and Title](#)

Wan XC, Steudle E, Hartung W (2004) Gating of water channels (aquaporins) in cortical cells of young corn roots by mechanical stimuli (pressure pulses): effects of ABA and of HgCl₂. Journal of Experimental Botany 55: 411-422

Pubmed: [Author and Title](#)

CrossRef: [Author and Title](#)

Google Scholar: [Author Only](#) [Title Only](#) [Author and Title](#)

Woodruff DR, McCulloh KA, Warren JM, Meinzer FC, Lachenbruch B (2007) Impacts of tree height on leaf hydraulic architecture and stomatal control in Douglas-fir. Plant Cell and Environment 30: 559-569

Pubmed: [Author and Title](#)

CrossRef: [Author and Title](#)

Google Scholar: [Author Only](#) [Title Only](#) [Author and Title](#)

Wu XQ, Lin JX, Lin QQ, Wang J, Schreiber L (2005) Casparian strips in needles are more solute permeable than endodermal transport barriers in roots of Pinus bungeana. Plant and Cell Physiology 46: 1799-1808

Pubmed: [Author and Title](#)

CrossRef: [Author and Title](#)

Google Scholar: [Author Only](#) [Title Only](#) [Author and Title](#)

Wylie RB (1947) Conduction in dicotyledon leaves The Proceedings of the Iowa Academy of Science 53: 195—202

Ye Q, Muhr J, Steudle E (2005) A cohesion/tension model for the gating of aquaporins allows estimation of water channel pore volumes in Chara. Plant Cell and Environment 28: 525-535

Pubmed: [Author and Title](#)

CrossRef: [Author and Title](#)

Google Scholar: [Author Only](#) [Title Only](#) [Author and Title](#)

Zhang YJ, Rockwell FE, Graham AC, Holbrook MN (2016) Reversible leaf xylem collapse: a potential 'circuit breaker' against cavitation. Plant Physiology doi:10.1104/pp.16.01191

Pubmed: [Author and Title](#)

CrossRef: [Author and Title](#)

Google Scholar: [Author Only](#) [Title Only](#) [Author and Title](#)